



Delft University of Technology
Faculty of Electrical Engineering, Mathematics and Computer Science
Faculty of Applied Sciences

**An Investigation into the Stabilization of Electrical
Power Grids Using a Second Order Kuramoto Model**

Thesis for
the faculties of EEMCS and Applied Sciences
fulfilling the requirements

of the degrees of

BACHELOR OF SCIENCE
in
APPLIED MATHEMATICS AND APPLIED PHYSICS

by

IAN LUIK

Delft, The Netherlands
June 2020

ABSTRACT

In this thesis different mechanisms of stabilizing a power grid are tested. The grid dynamics are modelled by a second order extension of the Kuramoto coupled oscillator model, also known as the swing equation. First we prove basic properties of the model such as periodicity and existence and uniqueness. Then we explore the properties of simple network topologies governed by the Kuramoto model. Finally we proceed to the testing of stabilization mechanisms. The stabilization mechanisms tested are (a) increasing the capacity of the power grid lines (b) implementing time delayed feedback mechanisms on the nodes and (c) decentralizing the power generation in the network. Moreover, we test whether examples of Braess' paradox, which states that adding an edge in a network can locally improve flow but globally cause congestion, can be found in a small network. Increasing the capacity of the power grid lines and implementing time delayed feedback are shown to have a positive effect on the stability of the grid. For a specific grid (the German power grid) it is shown that replacing a large power generator by many smaller generators can indeed have a positive effect on the stability, but this result has mediocre statistical certainty (p-value of 0.16). No instances have been found where removing a line from the network has a positive effect (Braess' paradox), however this is insufficient to conclude that no such instances exist.

Contents

1	INTRODUCTION	1
2	BASIC MODEL PROPERTIES	2
3	ANALYSIS OF BASIC NETWORK TOPOLOGIES	4
3.1	Two Nodes	4
3.2	N-Consumer Star Network	8
3.3	N-Consumer Cyclic Network	12
3.4	Influence of an Extra Line on the Stability of the Grid	18
4	LARGE NETWORK SIMULATIONS	20
4.1	Influence of Line Capacity on the Stability of the Grid	20
4.2	Influence of Feedback on the Stability of the Grid	25
4.3	Influence of Network Decentralization on the Stability of the Grid	28
5	CONCLUSIONS	30
	LIST OF REFERENCES	31

1 INTRODUCTION

This thesis covers research into the stability of electrical power grids and methods of stabilizing grids. In recent years, European grid operators have seen loads on their transmission cables increase as a result of increased electricity demand and renewable energy projects [1][2][3]. Loads increasing to near-maximum transmission capacities cause problems for keeping the power supply stable. For the German power grid, this problem is of such a magnitude that it requires active measures such as "installing phaseshifters on interconnectors" to "prevent neighbouring grids from being overwhelmed" [1]. These phaseshifters block loads from entering a different grid, but increase stability problems on Germany's own grid - they merely move the problem, instead of solving it.

The grid capacity issues are bound to increase in the future, because demand for electricity is expected to increase [4] in the European Union and because many new sustainable power generation projects are planned. It is thus essential to find ways of stabilizing the network when loads increase.

To test different methods of stabilizing power grids without integrating those methods physically (which would be infeasible economically), it is necessary to have a mathematical model that accurately approximates the behaviour of a real power grid. Such a model has been developed and studied [5] [6] [7]: it is a second order extension of the Kuramoto coupled oscillator model.

In this report, we use the second order Kuramoto model to answer to following question: what measures can be taken in order to increase the stability of a power grid?

The report starts with a treatment of the basic properties of the system of differential equations in chapter 3. After that, in chapter 3, basic topologies such as the star network and the cyclical network are analysed for the purposes of analytical insight and for reference in chapter 4. In chapter 3 we also explore the effect of removing a line in a small network. In chapter 4, we test three different methods for increasing stability: increasing cable capacity, active feedback-driven control systems and network decentralization. The report is wrapped up with a discussion of the conclusions in chapter 5.

This report is written as Bachelor thesis for the programs Applied Mathematics and Applied Physics at Delft University of Technology.

2 BASIC MODEL PROPERTIES

In this section we prove some basic properties of the model used throughout the text. The electrical power grid is modelled by a second order extension of the Kuramoto model. This second order model is also known as the swing equation.

The model is based on mechanical power transfer between machines. The machines are modelled as turbines that can produce, accumulate, dissipate and transfer energy.

For each node j , the time evolution of the system with initial phase $\phi_j(0) = \phi_{j,0}$ and initial frequency $\frac{d\phi_j}{dt}(0) = \omega_{j,0}$ (which physically represents the deviation from the common frequency of 50 Hz or 60 Hz) is governed by the system of ordinary differential equations $\frac{d^2\phi_j(t)}{dt^2} = \mathbf{f}(\phi(t), \frac{d\phi}{dt}(t))$, $\phi(t) \in \mathbb{R}^N$, $\mathbf{f} : \mathbb{R}^N \rightarrow \mathbb{R}^N$ where $f_j = \frac{d^2\phi_j(t)}{dt^2}$ is given by

$$\frac{d^2\phi_j(t)}{dt^2} = P_j - \alpha \frac{d\phi_j(t)}{dt} + \sum_{i=1}^N K_{ij} \sin(\phi_i(t) - \phi_j(t)) \quad j = 1, 2, \dots, N \quad (1)$$

where P_j is proportional to the amount of power produced or consumed by node j (where we choose $P_j \geq 0$ for producers and $P_j < 0$ for consumers), α is a damping term (for practical reasons, we consider within the scope of this paper α constant and equal for all nodes) and K_{ij} is a coupling constant proportional to the maximum power capacity of the transmission line between node i and node j . N denotes the number of nodes. In the remainder of this text we will omit writing down the t-dependence explicitly for reasons of brevity.

Furthermore, the total power production should equal the total power consumption. Thus the network should satisfy

$$\sum_j P_j = 0 \quad (2)$$

Classification The second order extension of the Kuramoto model is a second order non-linear autonomous system governed by a system of ordinary differential equations. Because much of the theory of ODEs assumes a first order ODE we will often rewrite the system as a system of $2N$ first order ODEs:

$$\begin{aligned} \frac{d\omega_j}{dt} &= P_j - \alpha\omega_j + \sum_{i=1}^N K_{ij} \sin(\phi_i - \phi_j) \\ \frac{d\phi_j}{dt} &= \omega_j \end{aligned} \quad (3)$$

Existence and Uniqueness For the model to be useful in making physical prediction, the initial value problem resulting from 3 equipped with initial conditions $\phi_j(0) = \phi_{j,0}$ and $\omega_j(0) = \omega_{j,0}$ needs to have a unique solution for any initial conditions. We therefore prove existence and uniqueness.

Theorem 2.1. Let $T \in [0, \infty)$ arbitrarily. Equation 3 has a unique solution for any initial conditions $\phi_j(0) = \phi_{j,0}$ and $\omega_j(0) = \omega_{j,0}$ on $[0, T]$.

We will state some known results without proof that we use to prove theorem 2.1.

Theorem 2.2. (Global existence and uniqueness, [8]) Consider the following initial value problem on \mathbb{R}^m : $\frac{d\mathbf{x}}{dt} = \mathbf{f}(\mathbf{x}, t)$, $\mathbf{x}(0) = \mathbf{x}_0$. Assume that $\mathbf{f}(\mathbf{x}, t)$ is piecewise continuous with respect to t . Furthermore, assume that for each $T \in [0, \infty)$ there exist finite constants k_T, h_T such that for all $t \in [0, T]$ $\mathbf{f}(\mathbf{x}, t)$ is globally Lipschitz continuous with Lipschitz constant k_T and $\forall t \in T \ |\mathbf{f}(\mathbf{x}_0, t)| \leq h_T$. Then the initial value problem has exactly one solution on $[0, T] \ \forall T \in [0, \infty)$.

Theorem 2.3. (Sufficient condition for Lipschitz continuity, [8]) Consider a function $\mathbf{f}(\mathbf{x}, t)$ that maps $\mathbb{R}^m \times \mathbb{R}^+ \rightarrow \mathbb{R}^m$. If $\forall i, j \in \mathbb{N} \cap [1, N]$ the partial derivative $\frac{\partial f_i(\mathbf{x}, t)}{\partial x_j}$ exists and its absolute value is bounded by a bound independent of \mathbf{x} , then $\mathbf{f}(\mathbf{x}, t)$ is globally Lipschitz with respect to \mathbf{x} .

Lemma 2.4. Let $\mathbf{x} \in \mathbb{R}^{2N}$ be defined by $[\omega_1 \omega_2 \dots \omega_N \phi_1 \phi_2 \dots \phi_N]^T$ and let $\mathbf{f}(\mathbf{x})$ be the function such that $\frac{d\mathbf{x}}{dt} = \mathbf{f}(\mathbf{x})$ as defined by equation 3. \mathbf{f} is globally Lipschitz continuous in \mathbf{x} .

Proof. (Lemma 2.4) By theorem 2.3 it suffices to show that all the absolute values of all partial derivatives are bounded by a bound independent of \mathbf{x} .

$$\begin{aligned} \left| \frac{\partial}{\partial \omega_k} \left(P_j - \alpha \omega_j + \sum_{i=1}^N K_{ij} \sin(\phi_i - \phi_j) \right) \right| &= \alpha \delta_{kj} \\ \left| \frac{\partial}{\partial \phi_j} \left(P_j - \alpha \omega_j + \sum_{i=1}^N K_{ij} \sin(\phi_i - \phi_j) \right) \right| &= \left| \sum_{i=1}^N K_{ij} \cos(\phi_i - \phi_j) \right| \leq \sum_{i=1}^N K_{ij} \\ \left| \frac{\partial}{\partial \phi_k} \left(P_j - \alpha \omega_j + \sum_{i=1}^N K_{ij} \sin(\phi_i - \phi_j) \right) \right| &= |K_{kj} \cos(\phi_k - \phi_j)| \leq K_{kj} \quad k \neq j \\ \left| \frac{\partial}{\partial \omega_k} (\omega_j) \right| &= \delta_{kj} \\ \left| \frac{\partial}{\partial \phi_k} (\omega_j) \right| &= 0 \end{aligned}$$

Indeed, all partial derivatives exist, its absolute values are bounded. The bounds are valid for the entire domain. So $\mathbf{f}(\mathbf{x})$ is Lipschitz continuous with respect to \mathbf{x} . \square

With these results the proof of theorem 2.1 becomes quite elementary.

Proof. (Theorem 2.1) Let $\mathbf{x} \in \mathbb{R}^{2N}$ be defined by $[\omega_1 \omega_2 \dots \omega_N \phi_1 \phi_2 \dots \phi_N]^T$ and let $\mathbf{f}(\mathbf{x})$ be the function such that $\frac{d\mathbf{x}}{dt} = \mathbf{f}(\mathbf{x})$ as defined by equation 3. Observe that the dynamical system is autonomous, so the piecewise continuous dependence of \mathbf{f} on t is trivial.

Let $T \in [0, \infty)$ and $t \in [0, T]$. Since the system is autonomous we only need to show the existence of finite constants k and h (independent of T) that satisfy the assumptions of theorem 2.2. The existence of k follows from lemma 2.4. The existence of h is easy to check since $\mathbf{f}(\mathbf{x}_0(t)) = \mathbf{f}(\mathbf{x}_0)$ which is well defined for all \mathbf{x} . The existence and uniqueness of the solution of the initial value problem follows from theorem 2.2. \square

Periodicity The phase space of the first order system is 2π -periodic in the ϕ_j -direction ($j = 1, 2, \dots, N$). This can be concluded from the fact that the tangent vector to a solution curve has a ϕ_j -dependence only in the term $\sum_{i=1}^N K_{ij} \sin(\phi_i - \phi_j)$ and replacing ϕ_j by $\phi_j + 2\pi k$ for any $k \in \mathbb{Z}$ has no effect.

Shift Symmetry The system is shift symmetric in the sense that replacing all ϕ_j by $\phi_j + \delta\phi$ has no effect on the dynamics of the system.

3 ANALYSIS OF BASIC NETWORK TOPOLOGIES

3.1 Two Nodes

We start our analysis by considering the stability of a two-node network with one generator g ($P_g \geq 0$) and one consumer c ($P_c < 0$). Let $P_g = P_0$ be the power produced by the generator. By equation 2 we must have $P_g = -P_0$. Using the fact that $K_{ij} = K_{ji}$ (there is only one transmission line between node i and j) we can fill out equation 1 for ϕ_g and ϕ_c and subtract the two in order to obtain

$$\frac{d^2\Delta\phi}{dt^2} = 2P_0 - \alpha\frac{d\Delta\phi}{dt} - 2K\sin(\Delta\phi) \quad (4)$$

where $K = K_{ij} = K_{ji}$ and $\Delta\phi = \phi_g - \phi_c$.

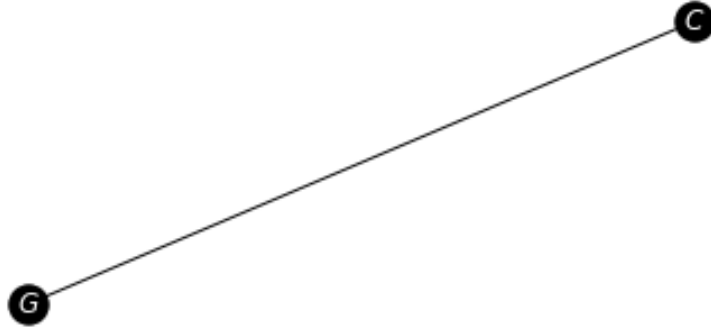


Figure 1: *Two node network, with G the generator and C the consumer.*

Required for the stable operation of this two-node network is the existence a stable equilibrium. In order to find the equilibrium points of this equation we separate the second-order ODE into two first-order ODEs:

$$\begin{aligned} \frac{d\Delta\phi}{dt} &= \omega \\ \frac{d\omega}{dt} &= 2P_0 - \alpha\omega - 2K\sin(\Delta\phi) \end{aligned} \quad (5)$$

Let $\mathbf{x} = [\Delta\phi, \omega]^T$. We can write this system of equations as $\frac{d\mathbf{x}}{dt} = \mathbf{f}(\mathbf{x})$. An equilibrium point x_0 is a point that satisfies $\mathbf{f}(\mathbf{x}_0) = \mathbf{0}$. The solutions for $\Delta\phi \in (-\pi, \pi]$ ¹ are $\omega = 0$ and, assuming $P_0 < K$,

$$\begin{aligned} \Delta\phi &= \arcsin\left(\frac{P_0}{K}\right) \\ \Delta\phi &= \pi - \arcsin\left(\frac{P_0}{K}\right) \end{aligned} \quad (6)$$

¹The restriction to $\Delta\phi \in (-\pi, \pi]$ is justified by the 2π -periodicity shown in chapter 2.

We prove that this equilibrium point is unstable using linearization around the equilibrium point, using the Hartman-Grobman theorem. Let $\mathbf{z} = \mathbf{x} - \mathbf{x}_0$. We can then write

$$\frac{d\mathbf{z}}{dt} = D[\mathbf{f}](\mathbf{x}_0)\mathbf{z} + O(|\mathbf{z}|^2) \quad (7)$$

By the Hartman-Grobman theorem, \mathbf{x}_0 is a stable equilibrium of equation 5 if x_0 is an unstable equilibrium point of the linearized system, i.e. if $D[\mathbf{f}](\mathbf{x}_0)$ has an eigenvalue λ_i with $Re\{\lambda_i\} < 0$. When computing the Jacobian matrix in the point $\mathbf{x}_0 = [\arcsin(\frac{P_0}{K}), 0]^T$ we obtain

$$D[\mathbf{f}](\mathbf{x}_0) = \begin{bmatrix} \frac{\partial f_1}{\partial \Delta\phi} & \frac{\partial f_1}{\partial \omega} \\ \frac{\partial f_2}{\partial \Delta\phi} & \frac{\partial f_2}{\partial \omega} \end{bmatrix}_{\mathbf{x}=\mathbf{x}_0} = \begin{bmatrix} 0 & 1 \\ -2K \cos(\arcsin(\frac{P_0}{K})) & -\alpha \end{bmatrix} = \begin{bmatrix} 0 & 1 \\ -2K\sqrt{1 - (\frac{P_0}{K})^2} & -\alpha \end{bmatrix} \quad (8)$$

resulting in

$$\lambda = -\frac{\alpha}{2} \pm \frac{1}{2} \sqrt{\alpha^2 - 8K\sqrt{1 - \left(\frac{P_0}{K}\right)^2}} \quad (9)$$

Assuming $K, P_0, \alpha > 0$ and $P_0 < K$ we can show that the real part of all eigenvalues are negative. First we consider the case $\alpha^2 \geq 8K\sqrt{1 - \left(\frac{P_0}{K}\right)^2}$ where $Re\{\lambda\} = \lambda$:

$$\lambda_{max} = -\frac{\alpha}{2} + \frac{1}{2} \sqrt{\alpha^2 - 8K\sqrt{1 - \left(\frac{P_0}{K}\right)^2}} < -\frac{\alpha}{2} + \frac{1}{2} \sqrt{\alpha^2} = 0 \quad (10)$$

In the other case where $\alpha^2 < 8K\sqrt{1 - \left(\frac{P_0}{K}\right)^2}$ both eigenvalues are complex with

$$Re\{\lambda\} = -\frac{\alpha}{2} < 0 \quad (11)$$

We conclude that $\Delta\phi = \arcsin(\frac{P_0}{K})$ is stable. In most practical cases α is small (meaning that the eigenvalues are complex), and thus $\Delta\phi = \arcsin(\frac{P_0}{K})$ is a stable spiral point. Now we consider the equilibrium $\mathbf{x}_0 = [\pi - \arcsin(\frac{P_0}{K}), 0]^T$. Following the same reasoning, we obtain

$$\lambda = -\frac{\alpha}{2} \pm \frac{1}{2} \sqrt{\alpha^2 + 8K\sqrt{1 - \left(\frac{P_0}{K}\right)^2}} \quad (12)$$

Both eigenvalues are real and

$$\lambda_{max} = -\frac{\alpha}{2} + \frac{1}{2} \sqrt{\alpha^2 + 8K\sqrt{1 - \left(\frac{P_0}{K}\right)^2}} > -\frac{\alpha}{2} + \frac{1}{2} \sqrt{\alpha^2} = 0 \quad (13)$$

It follows that this equilibrium point is unstable.

3.1.1 Limit Cycles

In the previous section it is shown that a two-node system has a stable equilibrium point $\omega = 0$, $\Delta\phi = \arcsin(\frac{P_0}{K})$. In figure 2 one can see that indeed, for certain initial conditions the trajectory converges to this equilibrium point, but for other initial conditions the trajectory converges to a limit cycle.

For $\frac{P_0}{K} > 1$, the equilibrium solution does not exist. In this case, one would expect all trajectories converge to a limit cycle. And for systems with a high damping factor α , physical intuition says that the equilibrium point should be globally stable. Figure 2 shows a situation where there is coexistence between the stable situation and limit cycles.

Definition 3.1. We call a system *globally stable* if for any initial conditions the trajectory converges to a stable equilibrium point.

Definition 3.2. We say that a system is in *coexistence* if (a) the system has a stable equilibrium point and (b) there exist initial conditions with trajectories converging to a limit cycle.

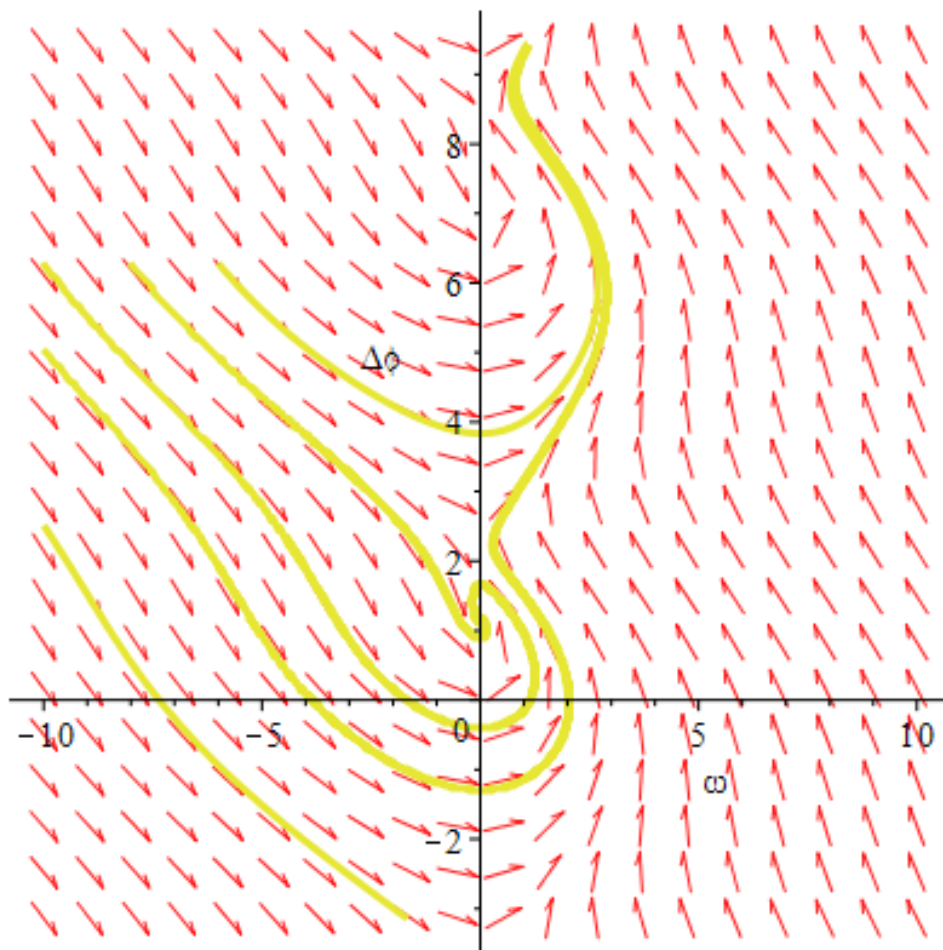


Figure 2: Phase portrait of a two-node system with $P_0 = 1$, $K = 1.1$, $\alpha = 1$. Several trajectories with varying initial conditions are drawn. Observe that some trajectories converge to a limit cycle, but two trajectories converge to the stable equilibrium point $(\omega, \Delta\phi) = (0, \arcsin(\frac{P_0}{K}))$. Thus with these parameters, the system is in a regime of coexistence between limit cycles and stable equilibria.

In this section, we show that for small α , the system is in coexistence for $P_0 \gtrsim \frac{4\alpha}{\sqrt{2}\pi} \sqrt{K}$ by showing that the system is mathematically analogous to an ideal pendulum (with gravity, a driving force and friction) and using the energy function of a pendulum to prove the claim.

Consider an ideal pendulum consisting of a point mass m and a massless rod with completely fixed length L . We use a polar coordinate system $(r, \Delta\phi)$ with the origin in the point of rotation and $\Delta\phi = 0$ if the vector between the origin and the point mass points parallel to the force of gravitation. Because the rod has fixed length, there is only a net force in the $\Delta\phi$ -direction. We therefore consider a scalar force balance in this direction only.

Suppose that the force of gravity acts on the point mass, as well as a constant force $2P_0mL$ and a friction force $-\alpha mL \frac{d\Delta\phi}{dt}$. Then by Newton's second law

$$mL \frac{d^2 \Delta\phi}{dt^2} = 2P_0mL - \alpha mL \frac{d\Delta\phi}{dt} - mg \sin(\Delta\phi) \quad (14)$$

and thus the original equation 4 follows with $2K = g/L$. A useful consequence of the physical analogy is that we can describe the energy function of the two-node network in the same way as the energy function of the pendulum, consisting of a kinetic and a potential term:

$$E = \frac{1}{2} \left(\frac{d\Delta\phi}{dt} \right)^2 - 2K \cos(\Delta\phi) \quad (15)$$

We determine the stability of the network using this energy function in Lyapunov's second method following [5]. If the energy averaged over period T decreases for all initial conditions² and all times, then the system is globally stable. Therefore to find the global stability criterion we need to solve

$$\frac{\overline{dE}}{dt} = 0 \quad (16)$$

Observe that if we apply the chain rule to equation 15 and substitute equation 4 we obtain

$$\begin{aligned} \frac{dE}{dt} &= \frac{d^2 \Delta\phi}{dt^2} \frac{d\Delta\phi}{dt} + 2K \sin(\Delta\phi) \frac{d\Delta\phi}{dt} \\ &= \left(2P_0 - \alpha \frac{d\Delta\phi}{dt} - 2K \sin(\Delta\phi) \right) \frac{d\Delta\phi}{dt} + 2K \sin(\Delta\phi) \frac{d\Delta\phi}{dt} \\ &= 2P_0 \frac{d\Delta\phi}{dt} - \alpha \left(\frac{d\Delta\phi}{dt} \right)^2 \end{aligned} \quad (17)$$

So we need to solve

$$0 = \frac{\overline{dE}}{dt} = \frac{1}{T} \int_{t_0}^{t_0+T} \left[2P_0 \frac{d\Delta\phi}{dt} - \alpha \left(\frac{d\Delta\phi}{dt} \right)^2 \right] dt \quad (18)$$

Using the fact that in one period T the phase changes by 2π :

$$\frac{1}{T} \int_0^T \frac{d\Delta\phi}{dt} dt = \frac{1}{T} \int_{\Delta\phi(t=t_0)}^{\Delta\phi(t=t_0)+2\pi} d\Delta\phi = \frac{2\pi}{T} \quad (19)$$

Rewriting equation 15 for $d\Delta\phi/dt$ we obtain

$$\begin{aligned} \frac{1}{T} \int_{t_0}^{T+t_0} \left(\frac{d\Delta\phi}{dt} \right)^2 dt &= \frac{1}{T} \int_{\Delta\phi(t_0)}^{\Delta\phi(t_0)+2\pi} \frac{d\Delta\phi}{dt} d\Delta\phi \\ &= \frac{1}{T} \int_{\Delta\phi(t_0)}^{\Delta\phi(t_0)+2\pi} \sqrt{2E(\Delta\phi, \frac{d\Delta\phi}{dt}) + 4K \cos(\Delta\phi)} d\Delta\phi \end{aligned} \quad (20)$$

and using that in the boundary case between global stability and the coexistence regime, $d\Delta\phi/dt = 0$ if and only if the potential is maximal, we can derive from equation 15 that $E_{peak_potential} = 2K$. In the small friction limit (a critical assumption that enables us to find an analytical solution to this problem), the energy can be assumed constant over a period. Thus we take $2E = 4K$ and

²A decrease of average energy for *all* initial conditions is critical, as this rules out the existence of limit cycles.

$$\frac{1}{T} \int_{t_0}^{T+t_0} \left(\frac{d\Delta\phi}{dt} \right)^2 dt = \frac{1}{T} \int_{\Delta\phi(t_0)}^{\Delta\phi(t_0)+2\pi} \sqrt{4K + 4K \cos(\Delta\phi)} d\Delta\phi = \frac{8\sqrt{2K}}{T} \quad (21)$$

substituting both results in equation 18 yields

$$\frac{2P_0 \cdot 2\pi}{T} - \frac{\alpha 8\sqrt{2K}}{T} = 0 \quad (22)$$

and we conclude the system is globally stable when $P_0 \lesssim \frac{4}{\sqrt{2\pi}} \alpha \sqrt{K}$. Otherwise the system is in coexistence.

3.2 N-Consumer Star Network

We generalize the two-node network to a network consisting of N consumers connected to one central generator with power P_0 . See figure 3.

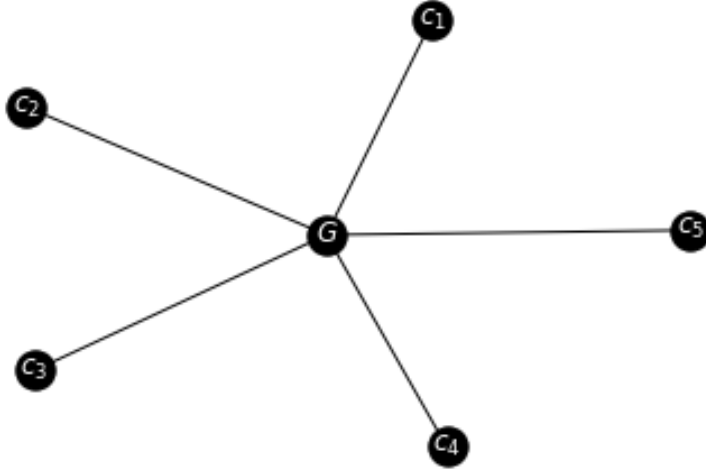


Figure 3: Example of a N-consumer star network, $N = 5$.

We assume all consumers take power $-\frac{P_0}{N}$ and all transmission lines have the same maximum power capacity K . Let ϕ_g denote the phase of the generator and let ϕ_{c_k} denote the phase of consumer k . This yields the system

$$\begin{aligned} \frac{d^2\phi_g}{dt^2} &= P_0 - \alpha \frac{d\phi_g}{dt} + K \sum_i \sin(\phi_{c_i} - \phi_g) \\ \frac{d^2\phi_{c_k}}{dt^2} &= -\frac{P_0}{N} - \alpha \frac{d\phi_{c_k}}{dt} + K \sin(\phi_g - \phi_{c_k}) \end{aligned} \quad (23)$$

We can fix ϕ_g freely, without loss of generality. We therefore transform the system to a system of N equations by defining

$$\Delta\phi_k = \phi_g - \phi_{c_k} \quad (24)$$

subtraction of the correct pairs of differential equations yields:

$$\frac{d^2 \Delta \phi_k}{dt^2} = P_0 \left(1 + \frac{1}{N}\right) - \alpha \frac{d \Delta \phi_k}{dt} - K \sum_{i=1}^N \sin(\Delta \phi_i) - K \sin(\Delta \phi_k) \quad (25)$$

We show that a stable equilibrium exists. For all $k \in \mathbb{N} \cap [1, N]$

$$\Delta \phi_k^* = \arcsin\left(\frac{P_0}{NK}\right) \vee \Delta \phi_k^* = \pi - \arcsin\left(\frac{P_0}{NK}\right) \quad (26)$$

for $|\frac{P_0}{NK}| \leq 1$. Denote the set of equilibrium points as E . Since $\{\arcsin(\frac{P_0}{NK}), \pi - \arcsin(\frac{P_0}{NK})\}^N \subseteq E$,

$$|E| \geq |\{\arcsin(\frac{P_0}{NK}), \pi - \arcsin(\frac{P_0}{NK})\}^N| = 2^N \quad (27)$$

We show that an equilibrium solution exists by showing $\Delta \phi_k^* = \arcsin(\frac{P_0}{NK}) \forall k \in \mathbb{N} \cap [1, N]$ is stable. We rewrite this system of N second-order differential equations into a system of N first-order ODEs:

$$\begin{aligned} \frac{d\omega_k}{dt} &= P - \alpha\omega_k - K \sum_i \sin(\Delta \phi_i) - K \sin(\Delta \phi_k) \\ \frac{d\Delta \phi_k}{dt} &= \omega_k \end{aligned} \quad (28)$$

where $P = P_0(1 + \frac{1}{N})$. Now we let

$$\mathbf{x} = \begin{bmatrix} \omega_1 \\ \Delta \phi_1 \\ \vdots \\ \omega_N \\ \Delta \phi_N \end{bmatrix} \quad (29)$$

and we write the system of equations as $\frac{d\mathbf{x}}{dt} = \mathbf{f}(\mathbf{x})$. By the Hartman-Grobman theorem it suffices to consider the eigenvalues of $D[\mathbf{f}]$ evaluated in the equilibrium point \mathbf{x}_0 . Let $c = K \cos(\arcsin(\frac{P_0}{NK})) = K \sqrt{1 - (\frac{P_0}{NK})^2}$.

$$\begin{aligned}
& D[\mathbf{f}](\mathbf{x}_0) \\
&= \begin{bmatrix} -\alpha & -2K \cos(\Delta\phi_1) & 0 & -K \cos(\Delta\phi_2) & 0 & -K \cos(\Delta\phi_3) & \dots & 0 & -K \cos(\Delta\phi_N) \\ 1 & 0 & 0 & 0 & 0 & 0 & \dots & 0 & 0 \\ 0 & -K \cos(\Delta\phi_1) & -\alpha & -2K \cos(\Delta\phi_2) & 0 & -K \cos(\Delta\phi_3) & \dots & 0 & -K \cos(\Delta\phi_N) \\ 0 & 0 & 1 & 0 & 0 & 0 & \dots & 0 & 0 \\ 0 & -K \cos(\Delta\phi_1) & 0 & -K \cos(\Delta\phi_2) & -\alpha & -2K \cos(\Delta\phi_3) & \dots & 0 & -K \cos(\Delta\phi_N) \\ 0 & 0 & 0 & 0 & 1 & 0 & \dots & 0 & 0 \\ \vdots & \vdots & \vdots & \vdots & \vdots & \vdots & \ddots & \vdots & \vdots \\ 0 & -K \cos(\Delta\phi_1) & 0 & -K \cos(\Delta\phi_2) & 0 & -K \cos(\Delta\phi_3) & \dots & -\alpha & -2K \cos(\Delta\phi_N) \\ 0 & 0 & 0 & 0 & 0 & 0 & \dots & 1 & 0 \end{bmatrix}_{\mathbf{x}=\mathbf{x}_0} \\
&= \begin{bmatrix} -\alpha & -2c & 0 & -c & 0 & -c & \dots & 0 & -c \\ 1 & 0 & 0 & 0 & 0 & 0 & \dots & 0 & 0 \\ 0 & -c & -\alpha & -2c & 0 & -c & \dots & 0 & -c \\ 0 & 0 & 1 & 0 & 0 & 0 & \dots & 0 & 0 \\ 0 & -c & 0 & -c & -\alpha & -2c & \dots & 0 & -c \\ 0 & 0 & 0 & 0 & 1 & 0 & \dots & 0 & 0 \\ \vdots & \vdots & \vdots & \vdots & \vdots & \vdots & \ddots & \vdots & \vdots \\ 0 & -c & 0 & -c & 0 & -c & \dots & -\alpha & -2c \\ 0 & 0 & 0 & 0 & 0 & 0 & \dots & 1 & 0 \end{bmatrix}
\end{aligned} \tag{30}$$

Theorem 3.1. The eigenvalues of $D[\mathbf{f}](\mathbf{x}_0)$ are

$$\begin{aligned}
\lambda &= -\frac{\alpha}{2} - \frac{1}{2}\sqrt{\alpha^2 - 4c} & a.m. N-1 \\
\lambda &= -\frac{\alpha}{2} + \frac{1}{2}\sqrt{\alpha^2 - 4c} & a.m. N-1 \\
\lambda &= -\frac{\alpha}{2} - \frac{1}{2}\sqrt{\alpha^2 - 4(N+1)c} & a.m. 1 \\
\lambda &= -\frac{\alpha}{2} + \frac{1}{2}\sqrt{\alpha^2 - 4(N+1)c} & a.m. 1
\end{aligned}$$

where a.m. is short for algebraic multiplicity.

Proof. We prove each eigenvalue separately, starting at $\lambda = -\frac{\alpha}{2} - \frac{1}{2}\sqrt{\alpha^2 - 4c}$. We prove that this is an eigenvalue by showing that

$$\begin{bmatrix} \frac{c}{\frac{\alpha}{2} - \frac{1}{2}\sqrt{\alpha^2 - 4c}} \\ -1 \\ -\frac{c}{\frac{\alpha}{2} - \frac{1}{2}\sqrt{\alpha^2 - 4c}} \\ 1 \\ 0 \\ 0 \\ \vdots \\ 0 \\ 0 \end{bmatrix}, \begin{bmatrix} \frac{c}{\frac{\alpha}{2} - \frac{1}{2}\sqrt{\alpha^2 - 4c}} \\ -1 \\ 0 \\ 0 \\ -\frac{c}{\frac{\alpha}{2} - \frac{1}{2}\sqrt{\alpha^2 - 4c}} \\ 1 \\ \vdots \\ 0 \\ 0 \end{bmatrix}, \dots, \begin{bmatrix} \frac{c}{\frac{\alpha}{2} - \frac{1}{2}\sqrt{\alpha^2 - 4c}} \\ -1 \\ 0 \\ 0 \\ 0 \\ 0 \\ \vdots \\ -\frac{c}{\frac{\alpha}{2} - \frac{1}{2}\sqrt{\alpha^2 - 4c}} \\ 1 \end{bmatrix}$$

are $(N-1)$ eigenvectors of $D[\mathbf{f}](\mathbf{x}_0)$.

$$\begin{bmatrix} -\alpha & -2c & 0 & -c & 0 & -c & \dots & 0 & -c \\ 1 & 0 & 0 & 0 & 0 & 0 & \dots & 0 & 0 \\ 0 & -c & -\alpha & -2c & 0 & -c & \dots & 0 & -c \\ 0 & 0 & 1 & 0 & 0 & 0 & \dots & 0 & 0 \\ 0 & -c & 0 & -c & -\alpha & -2c & \dots & 0 & -c \\ 0 & 0 & 0 & 0 & 1 & 0 & \dots & 0 & 0 \\ \vdots & \vdots & \vdots & \vdots & \vdots & \vdots & \ddots & \vdots & \vdots \\ 0 & -c & 0 & -c & 0 & -c & \dots & -\alpha & -2c \\ 0 & 0 & 0 & 0 & 0 & 0 & \dots & 1 & 0 \end{bmatrix} \begin{bmatrix} \frac{c}{\frac{\alpha}{2} - \frac{1}{2}\sqrt{\alpha^2 - 4c}} \\ -1 \\ -\frac{c}{\frac{\alpha}{2} - \frac{1}{2}\sqrt{\alpha^2 - 4c}} \\ 1 \\ 0 \\ 0 \\ \vdots \\ 0 \\ 0 \end{bmatrix} = \begin{bmatrix} -\alpha \frac{c}{\frac{\alpha}{2} - \frac{1}{2}\sqrt{\alpha^2 - 4c}} + 2c - c \\ \frac{c}{\frac{\alpha}{2} - \frac{1}{2}\sqrt{\alpha^2 - 4c}} \\ c + \alpha \frac{c}{\frac{\alpha}{2} - \frac{1}{2}\sqrt{\alpha^2 - 4c}} - 2c \\ -\frac{c}{\frac{\alpha}{2} - \frac{1}{2}\sqrt{\alpha^2 - 4c}} \\ c - c \\ 0 \\ \vdots \\ c - c \\ 0 \end{bmatrix} = \left(-\frac{\alpha}{2} - \frac{1}{2}\sqrt{\alpha^2 - 4c}\right) \begin{bmatrix} \frac{c}{\frac{\alpha}{2} - \frac{1}{2}\sqrt{\alpha^2 - 4c}} \\ -1 \\ -\frac{c}{\frac{\alpha}{2} - \frac{1}{2}\sqrt{\alpha^2 - 4c}} \\ 1 \\ 0 \\ 0 \\ \vdots \\ 0 \\ 0 \end{bmatrix}$$

The calculation for the other eigenvectors is analogous, so $\lambda = -\frac{\alpha}{2} - \frac{1}{2}\sqrt{\alpha^2 - 4c}$ is an eigenvalue of $D[\mathbf{f}](\mathbf{x}_0)$ with geometric multiplicity at least $N - 1$. It follows that the algebraic multiplicity is at least $N - 1$. The case $\lambda = -\frac{\alpha}{2} + \frac{1}{2}\sqrt{\alpha^2 - 4c}$ is analogous. Now we consider $\lambda = -\frac{\alpha}{2} - \frac{1}{2}\sqrt{\alpha^2 - (N+1)c}$ and show this is an eigenvalue:

$$\begin{bmatrix} -\alpha & -2c & 0 & -c & 0 & -c & \dots & 0 & -c \\ 1 & 0 & 0 & 0 & 0 & 0 & \dots & 0 & 0 \\ 0 & -c & -\alpha & -2c & 0 & -c & \dots & 0 & -c \\ 0 & 0 & 1 & 0 & 0 & 0 & \dots & 0 & 0 \\ 0 & -c & 0 & -c & -\alpha & -2c & \dots & 0 & -c \\ 0 & 0 & 0 & 0 & 1 & 0 & \dots & 0 & 0 \\ \vdots & \vdots & \vdots & \vdots & \vdots & \vdots & \ddots & \vdots & \vdots \\ 0 & -c & 0 & -c & 0 & -c & \dots & -\alpha & -2c \\ 0 & 0 & 0 & 0 & 0 & 0 & \dots & 1 & 0 \end{bmatrix} \begin{bmatrix} -\frac{(N+1)c}{\frac{\alpha}{2} - \frac{1}{2}\sqrt{\alpha^2 - 4(N+1)c}} \\ 1 \\ -\frac{(N+1)c}{\frac{\alpha}{2} - \frac{1}{2}\sqrt{\alpha^2 - 4(N+1)c}} \\ 1 \\ -\frac{(N+1)c}{\frac{\alpha}{2} - \frac{1}{2}\sqrt{\alpha^2 - 4(N+1)c}} \\ 1 \\ \vdots \\ -\frac{(N+1)c}{\frac{\alpha}{2} - \frac{1}{2}\sqrt{\alpha^2 - 4(N+1)c}} \\ 1 \end{bmatrix} = \begin{bmatrix} \alpha \frac{(N+1)c}{\frac{\alpha}{2} - \frac{1}{2}\sqrt{\alpha^2 - 4(N+1)c}} - 2c - (N-1)c \\ -\frac{(N+1)c}{\frac{\alpha}{2} - \frac{1}{2}\sqrt{\alpha^2 - 4(N+1)c}} \\ \alpha \frac{(N+1)c}{\frac{\alpha}{2} - \frac{1}{2}\sqrt{\alpha^2 - 4(N+1)c}} - 2c - (N-1)c \\ -\frac{(N+1)c}{\frac{\alpha}{2} - \frac{1}{2}\sqrt{\alpha^2 - 4(N+1)c}} \\ \alpha \frac{(N+1)c}{\frac{\alpha}{2} - \frac{1}{2}\sqrt{\alpha^2 - 4(N+1)c}} - 2c - (N-1)c \\ -\frac{(N+1)c}{\frac{\alpha}{2} - \frac{1}{2}\sqrt{\alpha^2 - 4(N+1)c}} \\ \vdots \\ \alpha \frac{(N+1)c}{\frac{\alpha}{2} - \frac{1}{2}\sqrt{\alpha^2 - 4(N+1)c}} - 2c - (N-1)c \\ -\frac{(N+1)c}{\frac{\alpha}{2} - \frac{1}{2}\sqrt{\alpha^2 - 4(N+1)c}} \end{bmatrix} = \left(-\frac{\alpha}{2} - \frac{1}{2}\sqrt{\alpha^2 - 4(N+1)c}\right) \begin{bmatrix} -\frac{(N+1)c}{\frac{\alpha}{2} - \frac{1}{2}\sqrt{\alpha^2 - 4(N+1)c}} \\ 1 \\ -\frac{(N+1)c}{\frac{\alpha}{2} - \frac{1}{2}\sqrt{\alpha^2 - 4(N+1)c}} \\ 1 \\ -\frac{(N+1)c}{\frac{\alpha}{2} - \frac{1}{2}\sqrt{\alpha^2 - 4(N+1)c}} \\ 1 \\ \vdots \\ -\frac{(N+1)c}{\frac{\alpha}{2} - \frac{1}{2}\sqrt{\alpha^2 - 4(N+1)c}} \\ 1 \end{bmatrix}$$

The case $\lambda = \left(-\frac{\alpha}{2} + \frac{1}{2}\sqrt{\alpha^2 - 4(N+1)c}\right)$ is analogous. We have yet to prove that the algebraic multiplic-

ities are $N - 1$, $N - 1$, 1 and 1 respectively. So far, we have only shown that the algebraic multiplicities are greater or equal to these values. Because

$$2N = (N - 1) + (N - 1) + 1 + 1 \leq \sum_i g.m.(\lambda_i) \leq \sum_i a.m.(\lambda_i) = \dim(D[\mathbf{f}](\mathbf{x}_0)) \leq 2N$$

we have equality. □

Corollary 3.1.1. The equilibrium solution \mathbf{x}_0 is stable if $|\frac{P_0}{NK}| < 1$.

3.3 N-Consumer Cyclic Network

Consider, instead of a star network, a cyclic network, where a generator g is connected to consumers c_1 and c_N and for $1 < i < N$ consumer c_i is connected to c_{i+1} and c_{i-1} . See figure 4. Rationale for exploring this network topology is that in practical neighbourhood network configurations, it can be expected that the most significant actors on the phase of a node (a house) are the node's neighbours and the large, central power supply.

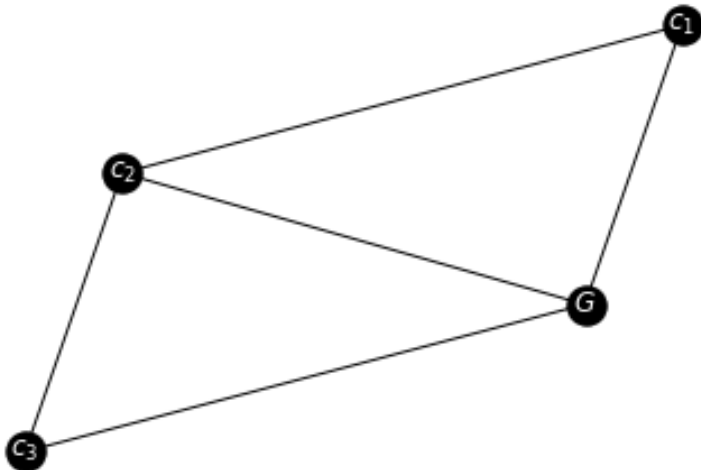


Figure 4: *Example of a N-consumer cyclic network, N = 3.*

We assume the generator generates a constant power P_0 and all consumers consume $-\frac{P_0}{N}$. We seek to explore the stability of equilibrium solutions of this network. In order to do so, we make a critical assumption: each consumer's phase is only influenced by the phases of its direct neighbors and the phase of the generator. We assume the generator's phase is influenced by the phases of all consumers. However, we do not assume that the consumer-consumer interactions and the consumer-generators are equally strong. Therefore, for the power transmission capacity we introduce two constants K_g and K_c . This

yields the following system of equations:

$$\begin{aligned}
\frac{d^2\phi_g}{dt^2} &= P_0 - \alpha \frac{d\phi_g}{dt} + K_g \sum_i \sin(\phi_{c_i} - \phi_g) \\
\frac{d^2\phi_{c_1}}{dt^2} &= -\frac{P_0}{N} - \alpha \frac{d\phi_{c_1}}{dt} + K_g \sin(\phi_g - \phi_{c_1}) + K_c \sin(\phi_{c_2} - \phi_{c_1}) \\
\frac{d^2\phi_{c_N}}{dt^2} &= -\frac{P_0}{N} - \alpha \frac{d\phi_{c_N}}{dt} + K_g \sin(\phi_g - \phi_{c_N}) + K_c \sin(\phi_{c_{N-1}} - \phi_{c_N}) \\
\frac{d^2\phi_{c_k}}{dt^2} &= -\frac{P_0}{N} - \alpha \frac{d\phi_{c_k}}{dt} + K_g \sin(\phi_g - \phi_{c_k}) + K_c (\sin(\phi_{c_{k+1}} - \phi_{c_k}) + \sin(\phi_{c_{k-1}} - \phi_{c_k}))
\end{aligned} \tag{31}$$

where $k \in \mathbb{N} \cap [2, N-1]$. Finding equilibrium solutions for this system of equations is significantly more complicated than before. Let us first consider the last equation from system 31. Solving the steady-state version of this equation yields

$$\phi_{c_{k-1}} = \phi_{c_k} + \arcsin \left(\frac{K_c N \sin(\phi_{c_k} - \phi_{c_{k+1}}) + K_g \sin(\phi_{c_k} - \phi_{c_g}) + P_0}{K_c N} \right) \tag{32}$$

and its result is visualized in figure 5. The figure shows that indeed ϕ_g can be fixed freely - as we shift ϕ_g by $\pi/2$, the holes (regions where there exists no equilibrium solutions) shift by $\pi/2$ in all other variables. This can be understood because the dynamics of the system depend only on the frequencies and the phase differences, but not on the phases itself.

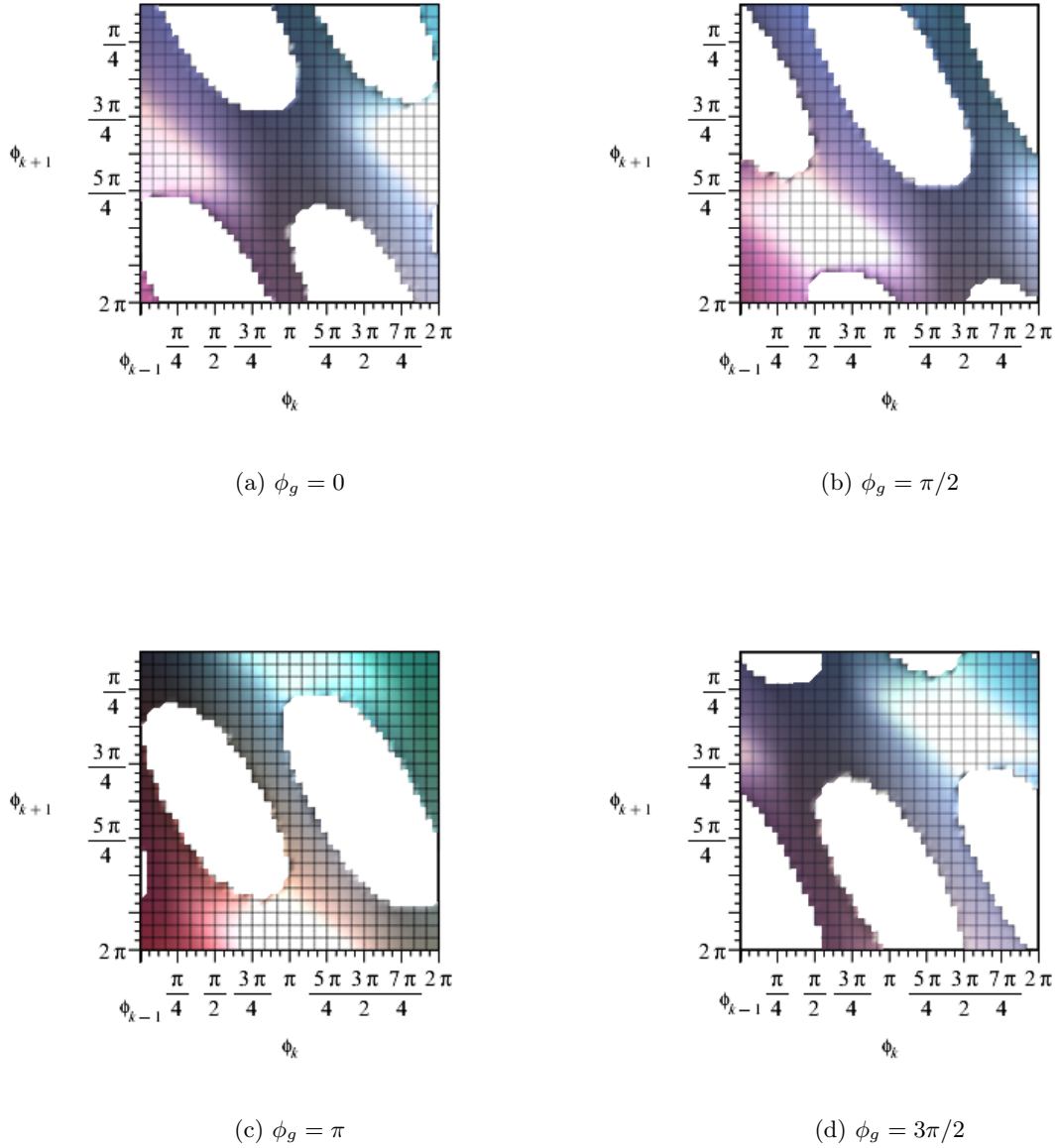


Figure 5: Plots of equation 32 for $K_g = K_c = P_0 = 1$, $N = 10$ and $\phi_g \in \{0, \pi/2, \pi, 3\pi/2\}$. The figures show the dependence of $\phi_{c_{k-1}}$ on ϕ_{c_k} and $\phi_{c_{k+1}}$. Both dependent variables have been plotted from 0 to 2π , as the phases are 2π -periodic. The holes indicate regions in the phase-space where no equilibrium solution exists.

3.3.1 3 Consumers

Because of the complexity of a general N-consumer system, we restrict the investigation to a 3-consumer cyclical network with one generator. This reduces the system of differential equations to:

$$\begin{aligned}
\frac{d^2\phi_g}{dt^2} &= P_0 - \alpha \frac{d\phi_g}{dt} + K_g \sum_{i=1}^3 \sin(\phi_{c_i} - \phi_g) \\
\frac{d^2\phi_{c_1}}{dt^2} &= -\frac{P_0}{3} - \alpha \frac{d\phi_{c_1}}{dt} + K_g \sin(\phi_g - \phi_{c_1}) + K_c \sin(\phi_{c_2} - \phi_{c_1}) \\
\frac{d^2\phi_{c_2}}{dt^2} &= -\frac{P_0}{3} - \alpha \frac{d\phi_{c_2}}{dt} + K_g \sin(\phi_g - \phi_{c_2}) + K_c (\sin(\phi_{c_3} - \phi_{c_2}) + \sin(\phi_{c_1} - \phi_{c_2})) \\
\frac{d^2\phi_{c_3}}{dt^2} &= -\frac{P_0}{3} - \alpha \frac{d\phi_{c_3}}{dt} + K_g \sin(\phi_g - \phi_{c_3}) + K_c \sin(\phi_{c_2} - \phi_{c_3})
\end{aligned} \tag{33}$$

The equilibrium solution depends on P_0 , K_g and K_c - but only on the ratios of these variables. Therefore, we can take $P_0 = 1$ without loss of generality. Furthermore, since we are only interested in relative phases, we take $\phi_g = 0$.

We find the equilibrium solutions of this system of equations by polynomial homotopy continuation, using the HomotopyContinuation package in the Julia programming language. This method requires the system of equations to be written as polynomials. To this end, we define $\sigma_i = \sin(\phi_{c_i})$ and $\gamma_i = \cos(\phi_{c_i})$ and use the identities $\sin(a - b) = \sin(a)\cos(b) - \cos(a)\sin(b)$ and $\sin^2(a) + \cos^2(b) = 1$ to rewrite the system in equilibrium with $\phi_g = 0$ as

$$\begin{aligned}
0 &= P_0 + K_g(\sigma_1 + \sigma_2 + \sigma_3) \\
0 &= -\frac{P_0}{3} - K_g\sigma_1 + K_c(\sigma_2\gamma_1 - \gamma_2\sigma_1) \\
0 &= -\frac{P_0}{3} - K_g\sigma_2 + K_c(\sigma_1\gamma_2 - \gamma_1\sigma_2 + \sigma_3\gamma_2 - \gamma_3\sigma_2) \\
0 &= -\frac{P_0}{3} - K_g\sigma_3 + K_c(\sigma_2\gamma_3 - \gamma_2\sigma_3) \\
1 &= \sigma_i^2 + \gamma_i^2 \quad i \in \{1, 2, 3\}
\end{aligned} \tag{34}$$

This is a system of polynomials which can be solved by the polynomial homotopy continuation method. This yields a set of equilibrium solution vectors $[\sigma_1^*, \sigma_2^*, \sigma_3^*, \gamma_1^*, \gamma_2^*, \gamma_3^*]^T$. Figure 6 shows bifurcation diagrams of the equilibrium solutions. We consider only the real solutions. This solution has to be transformed back to the ϕ_i^* that is of interest. This amounts to solving the system

$$\begin{aligned}
\sin(\phi_i^*) &= \sigma_i^* \quad i \in \{1, 2, 3\} \\
\cos(\phi_i^*) &= \gamma_i^* \quad i \in \{1, 2, 3\}
\end{aligned} \tag{35}$$

which yields

$$\phi_{c_i}^* = \arctan\left(\frac{\sigma_i^*}{\gamma_i^*}\right) + 2\pi n \quad i \in 1, 2, 3, n \in \mathbb{Z}, \sigma_i \neq 0 \tag{36}$$

We observe that the phase space is 2π -periodic in the ϕ_{c_i} -direction, as expected. Therefore we only plot from $-\pi$ to π . As ϕ_g^* has been fixed, all the remaining variables are consumer phases and frequencies. Thus we abbreviate ϕ_{c_k} to ϕ_k in the remainder of this section.

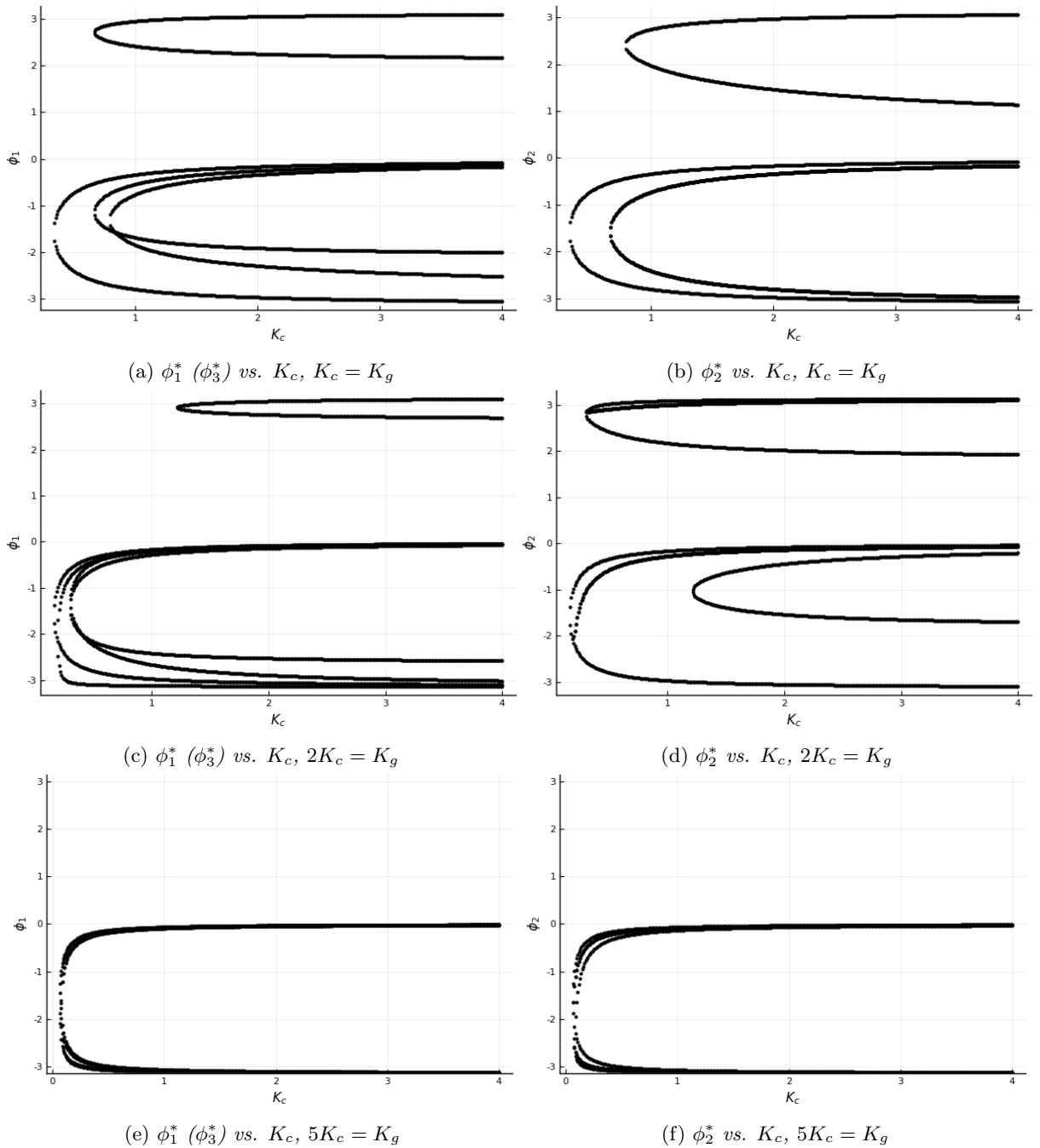
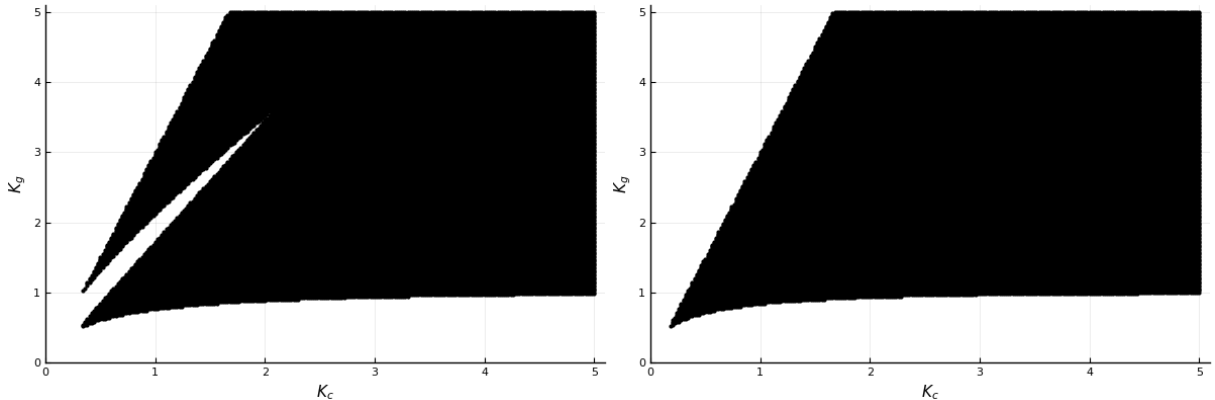


Figure 6: Bifurcation diagrams of the equilibrium solutions. The independent variable on the x-axis is K_g and the dependent variables are $\phi_1^* = \phi_3^*$ and ϕ_2^* . The solutions have been plotted for both $K_c = K_g$ and $2K_c = K_g$ and $5K_c = K_g$. An equilibrium solution ϕ consists of points ϕ_1^* , ϕ_3^* from plots 6a, 6c and 6e combined with some point from corresponding plots 6b, 6d and 6f. As we slowly increase the coupling constants K_g and K_c , the number of equilibrium solutions increases.

From figure 6, a few interesting conclusions can be drawn: firstly, the system is symmetric: if for a given K_c ϕ_1^* is the first component of some equilibrium solution, there exists an equilibrium solution with $\phi_3^* = \phi_1^*$ as the third component. Secondly, as one increases K_g , the number of equilibrium solutions increases from 0 to 2, to 4, to 6, to 8. The inner fork of ϕ_2^* has multiplicity 2, so there are only 4 unique ϕ_2^* -equilibrium points for high K_g . This makes sense from a physical point of view, since K_g and K_c are proportional to the line capacities. One would indeed expect more solutions with more power

transmission capacity.

Furthermore, it is apparent that as K_g increases compared to K_c the solution forks with $\phi_1^* \in [0, \pi]$, $\phi_2^* \in [0, \pi]$ and $\phi_3^* \in [0, \pi]$ disappear. This is to be expected as the $\frac{K_c}{K_g} \rightarrow 0$ limit corresponds to a star network which only has a fork in $[-\pi, 0]$. It is interesting to see how the existence of the forks in $[0, \pi]$ depend on the parameters K_g and K_c (where we still assume $P_0 = 1$ as this produces no qualitative difference). The regions where these forks exist are shown in figure 7.



(a) Region of existence of the forks with ϕ_1^* or $\phi_3^* \in [0, \pi]$ (b) Region of existence of the forks with $\phi_2^* \in [0, \pi]$

Figure 7: Diagrams showing the region of existence of the upper equilibrium forks as shown in figure 6.

A final observation is that an equilibrium solution always exists if $\frac{P_0}{3K_g} < 1$, namely a solution where $\phi_1^* = \phi_2^* = \phi_3^*$. In this case all terms with K_c in equation 33 become 0 and we are left with a star-network. Thus $\phi_1^* = \phi_2^* = \phi_3^* = \arcsin(\frac{P_0}{3K_g})$ is an equilibrium solution. To find out whether this solution is stable, we use the same approach that was used for the star-network: write $\mathbf{x} = [\omega_1, \Delta\phi_1, \omega_2, \Delta\phi_2, \omega_3, \Delta\phi_3]^T$ with $\Delta\phi_k = \phi_g - \phi_{c_k}$. Then we rewrite equation 33 as

$$\begin{aligned}
 \frac{d\omega_1}{dt} &= \frac{4}{3}P_0 - \alpha\omega_1 - K_g \sum_{i=1}^3 \sin(\Delta\phi_i) - K_g \sin(\Delta\phi_1) + K_c \sin(\Delta\phi_2 - \Delta\phi_1) \\
 \frac{d\Delta\phi_1}{dt} &= \omega_1 \\
 \frac{d\omega_2}{dt} &= \frac{4}{3}P_0 - \alpha\omega_2 - K_g \sum_{i=1}^3 \sin(\Delta\phi_i) - K_g \sin(\Delta\phi_2) + K_c \sin(\Delta\phi_1 - \Delta\phi_2) + K_c \sin(\Delta\phi_3 - \Delta\phi_2) \\
 \frac{d\Delta\phi_2}{dt} &= \omega_2 \\
 \frac{d\omega_3}{dt} &= \frac{4}{3}P_0 - \alpha\omega_3 - K_g \sum_{i=1}^3 \sin(\Delta\phi_i) - K_g \sin(\Delta\phi_3) + K_c \sin(\Delta\phi_2 - \Delta\phi_3) \\
 \frac{d\Delta\phi_3}{dt} &= \omega_3
 \end{aligned} \tag{37}$$

which defines a differential equation $\frac{d\mathbf{x}}{dt} = \mathbf{f}(\mathbf{x})$ with corresponding Jacobian (in the equilibrium solution)

$$D[\mathbf{f}(\mathbf{x}^*)] = \begin{bmatrix} -\alpha & -2c - K_c & 0 & -c + K_c & 0 & -c \\ 1 & 0 & 0 & 0 & 0 & 0 \\ 0 & -c + K_c & -\alpha & -2c - 2K_c & 0 & -c + K_c \\ 0 & 0 & 1 & 0 & 0 & 0 \\ 0 & -c & 0 & -c + K_c & -\alpha & -c - K_c \\ 0 & 0 & 0 & 0 & 1 & 0 \end{bmatrix} \quad (38)$$

with $c = K_g \cos(\arcsin(\frac{P_0}{3K})) = K_g \sqrt{1 - (\frac{P_0}{3K})^2}$. The corresponding eigenvalues are

$$\begin{aligned} \lambda_1 &= -\frac{\alpha}{2} - \frac{1}{2}\sqrt{\alpha^2 - 16c} \\ \lambda_2 &= -\frac{\alpha}{2} + \frac{1}{2}\sqrt{\alpha^2 - 16c} \\ \lambda_3 &= -\frac{\alpha}{2} - \frac{1}{2}\sqrt{\alpha^2 - 4K_c - 4c} \\ \lambda_4 &= -\frac{\alpha}{2} + \frac{1}{2}\sqrt{\alpha^2 - 4K_c - 4c} \\ \lambda_5 &= -\frac{\alpha}{2} - \frac{1}{2}\sqrt{\alpha^2 - 12K_c - 4c} \\ \lambda_6 &= -\frac{\alpha}{2} + \frac{1}{2}\sqrt{\alpha^2 - 12K_c - 4c} \end{aligned} \quad (39)$$

Observe that all eigenvalues have a negative real part, since c is always positive and $K_c \geq 0$. Thus the solution is stable.

We have shown that the stability of this equilibrium solution is dependent on the ratio's between P_0 , K_g and independent of K_c and α . For all the other equilibrium points we have no exact solution, so such an analysis is infeasible. But likely their stability depends on P_0 , K_g and K_c , and finding out the stability criteria (numerically) of the other equilibrium solutions would be an interesting topic for further research.

3.4 Influence of an Extra Line on the Stability of the Grid

An additional question to be asked about this topology is: what is the effect of removing a line from the network. Braess' paradox says that removing a connection in a graph might globally improve the flow. It has been shown in [9] that Braess' paradox occurs in traffic networks: for certain traffic parameters, adding a new road to the network decreases travel time locally, but increases congestion globally.

In the context of power grid, Braess' paradox can be formulated differently: could adding a line to the network influence the power flow in such a way that it actually decreases the number of equilibrium solutions? Thus we try to find an example in the 3-consumer network where removing a line - say the line between the generator and consumer 2 - has a positive effect on the number of equilibrium solutions. The proposed line removal changes the network to a pure cyclic network. The network is shown in figure 8. The resulting bifurcation diagram is shown in figure 9.

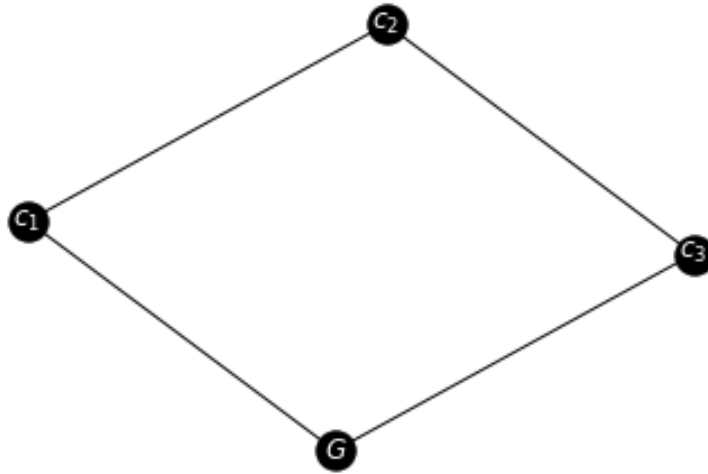


Figure 8: *Example of a N -consumer cyclic network, $N = 3$.*

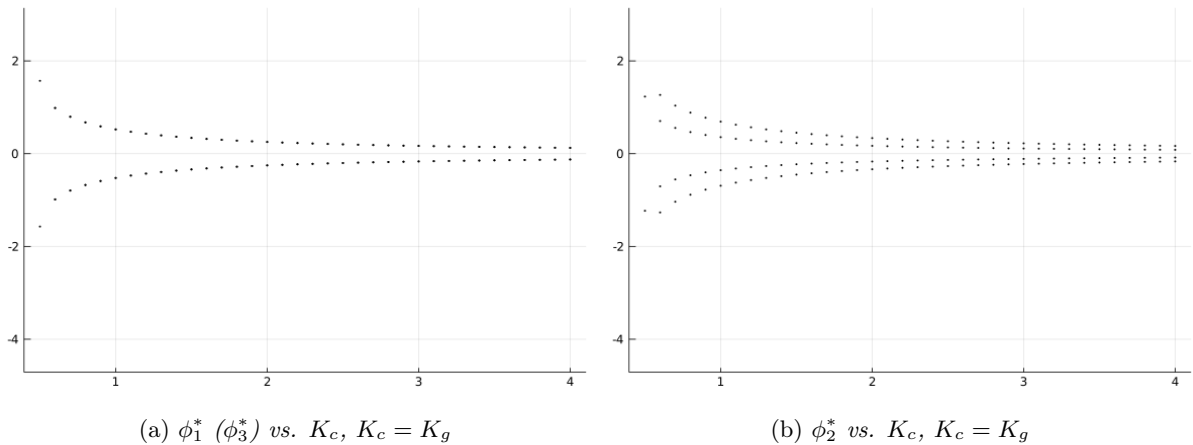


Figure 9: *Bifurcation diagrams of equilibrium solutions for the 3-consumer network without a link between the generator and consumer 2.*

Observe that the number of solutions is lower for this network - at $K_c = K_g = 4$ we have only 4 solutions instead of 8. The same result holds qualitatively for other power configurations such as $\{P_G, P_{c_1}, P_{c_2}, P_{c_3}\} = \{P_0, P_0, -P_0, -P_0\}, \{P_0, -P_0, P_0, -P_0\}$. No example has been found on the 3-consumer network where removing a line has a positive effect on the number of equilibrium solutions. It is possible however, that certain configurations do show Braess' paradox. In this piece of research no conclusive answer to this matter has been found.

4 LARGE NETWORK SIMULATIONS

In this chapter, larger power grids are simulated numerically, following partially the work done by Taher, Olmi and Schöll in [6] and using the Open Source Electricity Model for Germany (ELMOD-DE) [10].

In order to have a Kuramoto model that can handle real world power data we cast equation 1 in a different form:

$$\frac{d^2\phi_j}{dt^2} = \frac{P_j}{I_j\omega_g} - \alpha \frac{d\phi_j}{dt} + \sum_{i=1}^N \frac{K_{ij}}{I_j\omega_g} \sin(\phi_i - \phi_j) \quad (40)$$

or, written as a system of first-order equations:

$$\begin{aligned} \frac{d\omega_j}{dt} &= \frac{P_j}{I_j\omega_g} - \alpha\omega_j + \sum_{i=1}^N \frac{K_{ij}}{I_j\omega_g} \sin(\phi_i - \phi_j) \\ \frac{d\phi_j}{dt} &= \omega_j \end{aligned} \quad (41)$$

where P_j [W] is the power produced by node j , I_j [kg m²] is the moment of inertia of turbine j (the Kuramoto model is derived from a physical turbine system) and ω_g is the reference frequency of the power grid. The reason for casting the equation in this form is that P_j now physically represents power, instead of merely representing an abstract mathematical variable proportional to power. Indeed, checking the units we find that the unit of $[\frac{P_j}{I_j\omega_g}]$ is s⁻², which is equal to the unit of $\frac{d^2\phi_j}{dt^2}$.

4.1 Influence of Line Capacity on the Stability of the Grid

4.1.1 Model and Assumptions

The ELMOD-DE model provides a network consisting of $N = 438$ nodes holding a total of 562 power plants. Moreover, it provides an adjacency matrix that indicates which nodes are connected by power lines. As the model represents only Germany's high-power grid, we can assume that the nodes are connected by similar cables. Thus we define $K_{ij} = KA_{ij}$ where $A_{ij} = 1$ if there is a cable between node i and j and 0 otherwise³. In this section, we focus on the influence of the line capacity on the stability of the grid. Thus we leave K as variable parameter and use for the other parameters the values provided by Taher, Olmi and Schöll: $\alpha = \frac{5}{6} \text{ s}^{-1}$, $I_j = I = 40 \cdot 10^3 \text{ kg m}^2$ and $\omega_g = 2\pi \cdot 50 \text{ s}^{-1}$.

The values of P_j are yet to be specified. The ELMOD-DE-data give fractional demand powers $p_j \in [0, 1]$ of the total demanded power P_{total} with $j \in \mathbb{N} \cap [1, N]$ such that

$$\sum_{j=1}^N p_j = 1 \quad (42)$$

Furthermore, the dataset specifies power plant capacities for all the power plants. For each node j we compute its production capacity C_j by taking the sum of the capacities of the corresponding power plants. We assume each plant operates at the same fraction of its capacity. Finally we require that the total power production is equal to the total power consumption, so we define an operation rate $c_j \in [0, 1]$ such that

$$P_{total} = \sum_{j=1}^N c_j C_j \quad (43)$$

³Observe that this definition leaves ambiguity regarding the value of the diagonal elements A_{ii} . We do not, however, bother choosing values for the diagonal elements since their products with $\sin(\phi_i - \phi_i)$ are all 0 regardless of their values.

and we assume that $c_j = c = P_{total} / \sum_{i=1}^N C_i$. It finally follows that

$$P_j = cC_j - p_j P_{total} \quad (44)$$

The numerical values are $P_{total} = 36$ GW and $\sum_{j=i}^N C_i = 88.354$ GW.

4.1.2 Simulations and Results

We generate random initial conditions ϕ_j and $\omega_j = \frac{d\phi_j}{dt}$ with $\phi_j, \omega_j \sim N(0; 1)$ and then simulate the network for 25 s with time steps of 0.01 s for K ranging from 300 MW to 2400 MW in steps of 300 MW. The time evolution graphs of nodal frequencies are shown in figure 10. The empirical means and standard deviations of the nodal frequencies after 25 s are listed in table 1.

Firstly, observe that the system becomes more ordered as K increases. This is to be expected as K functions as coupling parameter. Secondly, note that there is a large number of different limit cycles. This is a phenomenon that can be understood from the earlier results from the small network analysis. In that chapter we have shown that the existence of limit cycles depends on the ratio between the net power production and the transmission line capacity. As the net power production and the total transmission line capacity is different for different nodes, it is to be expected that there exist a multitude of equilibrium solutions and limit cycles.

Thirdly, observe that the mean frequency after 25 s has the same non-zero value for all K tested. It can easily be shown that that $\bar{\omega}(t)$ is independent of K . In fact, this holds in a more general setting - it suffices to assume $K_{ij} = K_{ji} \wedge I_i = I_j \forall i, j \in \mathbb{N} \cap [1, N]$, which is true for all physical situations.

$$\begin{aligned} \frac{d\bar{\omega}}{dt} &= \frac{1}{N} \sum_{j=1}^N \frac{d\omega_j}{dt} = \frac{1}{N} \sum_{j=1}^N \left[\frac{P_j}{I_j \omega_g} - \alpha \omega_j + \sum_{i=1}^N \frac{K_{ij}}{I_j \omega_g} \sin(\phi_i - \phi_j) \right] \\ &= \frac{1}{N} \sum_{j=1}^N \sum_{i=1}^N \left[\frac{P_j}{I_j \omega_g} - \alpha \omega_j + \frac{K_{ij}}{I_j \omega_g} \sin(\phi_i - \phi_j) \right] = \frac{1}{N} \sum_{j=1}^N \sum_{i=1}^N \left[\frac{P_j}{I_j \omega_g} - \alpha \omega_j \right] \end{aligned} \quad (45)$$

In the last equality we used $K_{ij} = K_{ji}$ and $\sin(\phi_j - \phi_i) = -\sin(\phi_i - \phi_j)$. The derivative of $\bar{\omega}(t)$ is independent of K and so is $\bar{\omega}(0)$. We conclude that the ensemble average of the frequencies is indeed independent of K .

Table 1: Empirical mean and standard deviation of the nodal frequencies ω_j at $t = 25s$.

K [MW]	Mean [s⁻¹]	Standard Deviation [s⁻¹]
300	0.039243684598	15.0924402836
600	0.039243684598	6.15963372552
900	0.039243684598	4.76994876474
1200	0.039243684598	1.66321898266
1500	0.039243684598	1.38817864654
1800	0.039243684598	6.0771157283 · 10 ⁻⁸
2100	0.039243684598	7.52449774193 · 10 ⁻⁸
2400	0.039243684598	3.64306801636 · 10 ⁻⁸

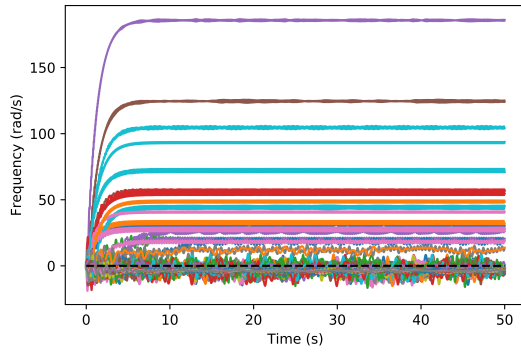
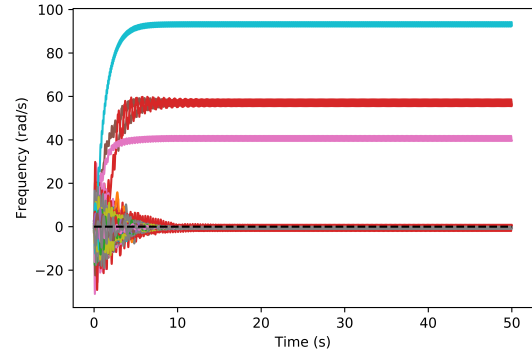
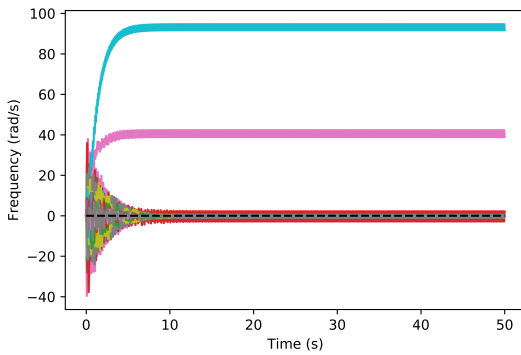
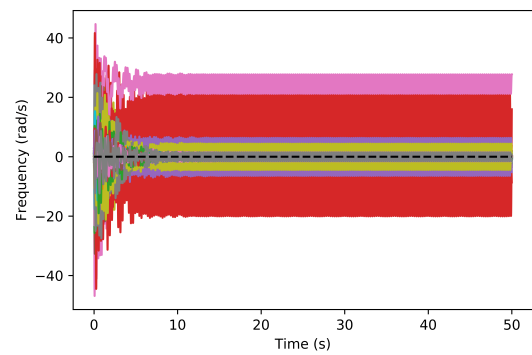
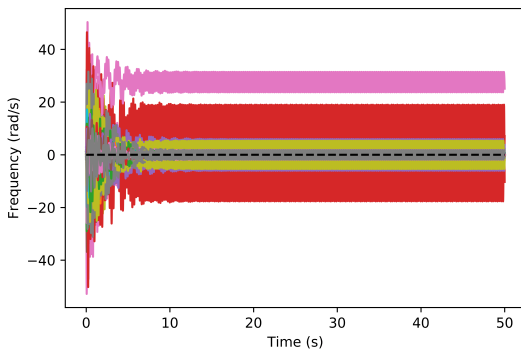
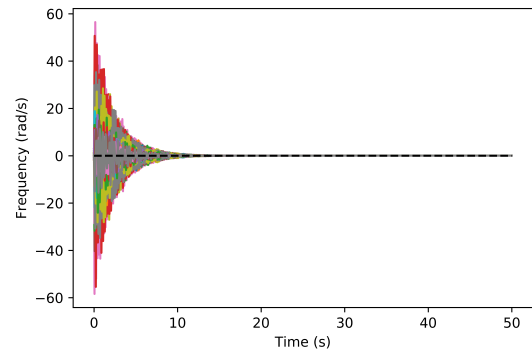
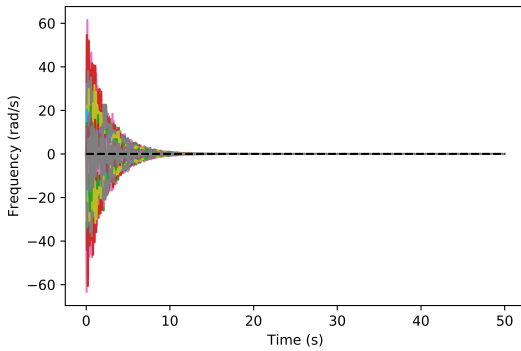
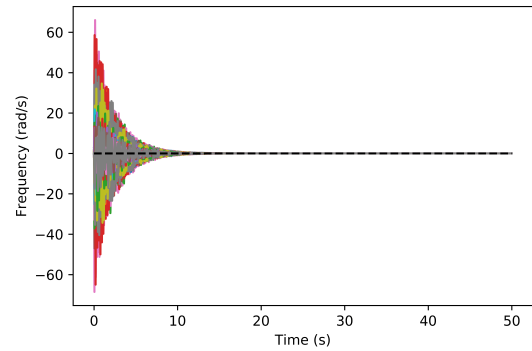
(a) $K = 300 \text{ MW}$ (b) $K = 600 \text{ MW}$ (c) $K = 900 \text{ MW}$ (d) $K = 1200 \text{ MW}$ (e) $K = 1500 \text{ MW}$ (f) $K = 1800 \text{ MW}$ (g) $K = 2100 \text{ MW}$ (h) $K = 2400 \text{ MW}$

Figure 10: Graphs showing the evolution of the nodal frequencies ω_j in time for $K = 300 \text{ MW}$ to $K = 2400 \text{ MW}$. The black dashed line indicates $\omega = 0$. Note that convergence to $\omega = 0$ is to be expected for high K , as ω represents the deviation from the common frequency (50 Hz or 60 Hz).

It is however, strange from a physical point of view that even for high values K where all the frequencies seem to converge to a single constant value, the frequencies do not tend to 0. Even though the frequencies represent in reality only the deviations from 50Hz . One would presume that this is either an artefact of this network under the Kuramoto model (that with these in initial conditions on this particular network the frequency deviations do not converge to 0) or that it is a numerical issue.

Phase Ordering Figure 10 demands a further analysis of the phase ordering of the network. According to [7] the phase ordering can be characterized by a phase order parameter $r(t) = \frac{1}{N} \sum_{j=1}^N e^{i\phi_j(t)}$ where $|r(t)| = 1$ describes complete synchronization and $|r(t)| = 0$ describes a completely asynchronous state. The asymptotic synchronization is measured by

$$r_\infty = \lim_{t \rightarrow \infty} \frac{1}{T} \int_t^{t+T} r(s) ds \quad (46)$$

assuming a sufficiently large value of T .

The phase order parameters $r(t)$ have been computed for the previously mentioned values of K and its absolute values are shown in figure 11. $|r_\infty|$ is estimated by taking $t = 45$ s and $T = 5$ s. Its values are shown in table 2.

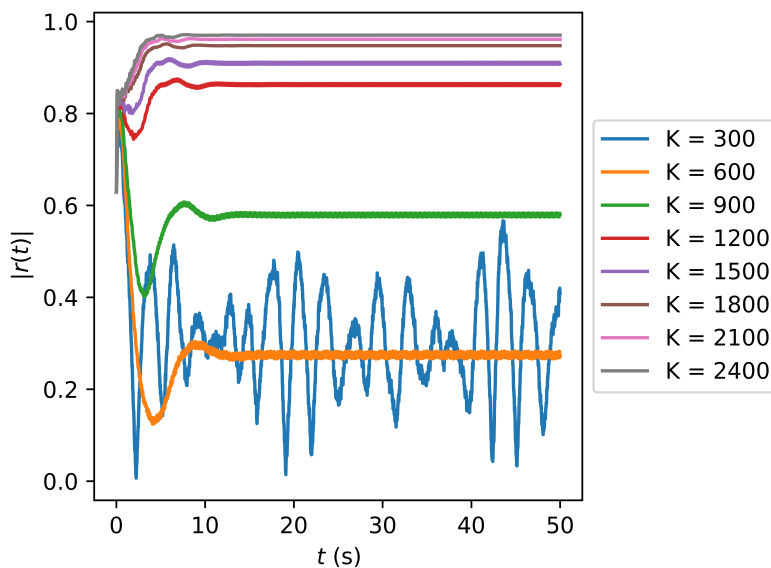


Figure 11: $r(t)$ plotted for various values of K .

Table 2: Asymptotic phase ordering parameters for various values of K .

K [MW]	300	600	900	1200	1500	1800	2100	2400
$ r_\infty $	0.3040	0.2752	0.5789	0.8622	0.9089	0.9475	0.9613	0.9703

Note that the ordering parameter increases for increasing values of K . For very low values of K , the phase ordering itself might not converge. For higher values of K , the phase ordering converges, but not necessarily to 1, indicating that some degree of asymmetry is still present in the system.

Lyapunov characteristic exponent Another characteristic number that indicates the level of order or chaos in a dynamical system is the maximum Lyapunov exponent λ_{max} , which characterizes the divergence rate of two trajectories that start infinitesimally close together [11]. It is computed by taking two initial conditions \mathbf{x}_0 and $\mathbf{x}_0 + \delta\mathbf{x}_0$ and taking the following limit:

$$\lambda_{max} = \lim_{t \rightarrow \infty} \lim_{\delta\mathbf{x}_0 \rightarrow 0} \frac{1}{t} \ln \left(\frac{|\delta\mathbf{x}(t)|}{|\delta\mathbf{x}_0|} \right) \quad (47)$$

We explore the dependence of λ_{max} on the coupling parameter K by using an upsweep and downsweep algorithm. It works as follows: start at some initial value for $K_{initial}$ and the network simulate for a transient time $T_{transient}$ time by with random initial conditions. Then take the final value of $\mathbf{x}(t)$ in this time interval as initial condition for the next interval. Increase K by a step ΔK and simulate again for a time $T_{transient}$. Repeat this until the value of K reached some K_{max} where the system is (by approximation) fully synchronized. The entire procedure so far is the upsweep part of the algorithm and had the purpose of finding an equilibrium solution from which we can perturb the system slightly in order to estimate λ_{max} .

The algorithm continues by going in the reverse direction. We decrease K by ΔK and simulate the trajectory of initial condition \mathbf{x}_0 for time $T_{transient}$, as well as the trajectory of $\mathbf{x}_0 + \delta\mathbf{x}_0$ for some small $\delta\mathbf{x}_0$. We then generate an estimate $\tilde{\lambda}_{max}$ of λ_{max} using the formula

$$\tilde{\lambda}_{max} = \frac{1}{T_{Transient}} \ln \left(\frac{|\delta\mathbf{x}(T_{transient})|}{|\delta\mathbf{x}_0|} \right) \quad (48)$$

We keep repeating these steps, each time decreasing K by ΔK up until some point $K_{intermediate}$, chosen such that it is just above the value of K where the system loses stability. Then the step size of K is decreased to a value ΔK_{small} and the algorithm continues until a value K_{final} is reached. The values used are shown in table 3.

Table 3: *Parameters used for the computation of $\tilde{\lambda}_{max}(K)$*

Quantity [Unit]	Value
$K_{initial}$ [MW]	900
K_{max} [MW]	9000
$K_{intermediate}$ [MW]	500
K_{final} [MW]	100
ΔK [MW]	250
ΔK_{small} [MW]	5
$T_{Transient}$ [s]	50
dt [s]	0.02
$\delta\mathbf{x}_0$ [rad, rad/s]	$\pm 10^{-6}$

The estimates of the maximum Lyapunov exponents are shown in figure 12. Observe that the system seems to be stable from $K \approx 370$ MW, as from this point forward the MLE's are approximately 0, meaning that the curves do not diverge. The estimates are not exactly zero, but this might very well be caused by numerical errors.

Because of the shift symmetry (all phases can be shifted by some constant $\delta\phi$) there is a Lyapunov exponent of 0 in the spectrum. This can be understood because the Lyapunov exponent characterizes the evolution of the separation of trajectories in the following way: let $\mathbf{x}_1(0), \mathbf{x}_2(0)$ be two initial conditions sufficiently close together for the linear approximation to hold. Then for the separation vector $\delta\mathbf{x} = \mathbf{x}_1 - \mathbf{x}_2$

$$|\delta\mathbf{x}(t)| \approx e^{\lambda_{max}t} |\delta\mathbf{x}(0)| \quad (49)$$

and if the two initial conditions only differ in the phase part of the vector space by a phase difference of $\delta\phi$, both trajectories have constant separation: $\delta\mathbf{x}(t) = \mathbf{x}(0) \forall t \geq 0$ and thus $\lambda_{max} = 0$. So if figure 12 shows that $\lambda_{max} = 0$, it could mean that two trajectories with truly different initial conditions (meaning a difference other than a uniform shift in phase) would converge. If this is the case, the equilibrium is stable.

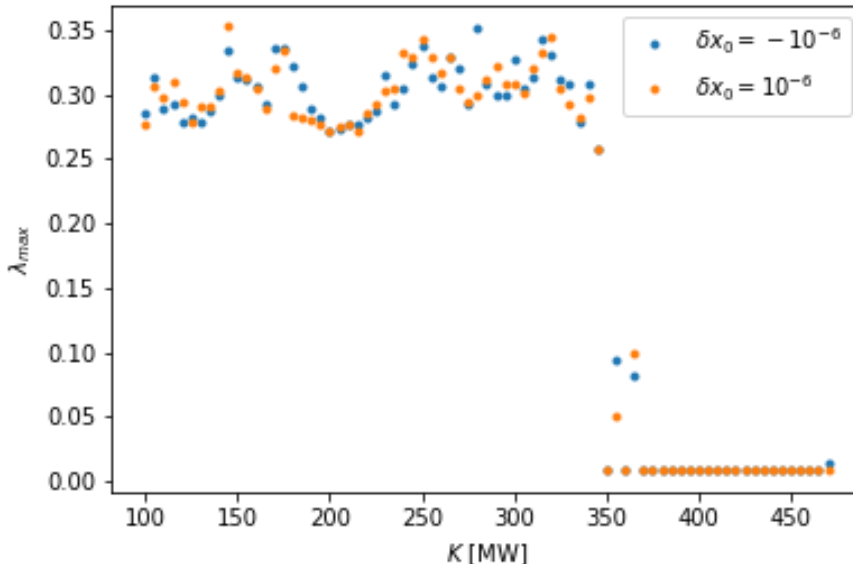


Figure 12: $\tilde{\lambda}_{max}$ plotted for various values of K

4.2 Influence of Feedback on the Stability of the Grid

In [6] a feedback system is proposed to enhance the stability of the power grid where for a subset of the nodes in the grid the differential equation is modified to

$$\frac{d^2\phi_j(t)}{dt^2} = P_j - \alpha \frac{d\phi_j(t)}{dt} + \sum_{i=1}^N K_{ij} \sin(\phi_i(t) - \phi_j(t)) - \frac{g_i\alpha}{\tau} (\phi_j(t) - \phi_j(t - \tau)) \quad (50)$$

where g_i is a gain parameter and τ is the delay time. This modification changes the system to a system of delay differential equations.

Firstly, observe that this modification does not effect existence or the values of the equilibrium solutions: if ϕ^* is an equilibrium solution of the regular system, then $\phi_j^*(t) = \phi_j^*(t - \tau)$ and the feedback terms vanish.

Secondly, note that $\lim_{\tau \rightarrow 0} \frac{\phi_j(t) - \phi_j(t - \tau)}{\tau} = \frac{d\phi_j(t)}{dt}$ and thus in the $\tau \rightarrow 0$ limit we simply obtain a more heavily damped system:

$$\frac{d^2\phi_j(t)}{dt^2} = P_j - (1 + g_i)\alpha \frac{d\phi_j(t)}{dt} + \sum_{i=1}^N K_{ij} \sin(\phi_i(t) - \phi_j(t)) \quad (51)$$

It would thus follow that at least for systems with small delay times the system is more robust to perturbations around equilibrium solutions - that is, the size of the basin of stability is increased. Unfortunately, solving DDE's numerically is much more computationally intensive than solving ODE's. It is therefore infeasible to simulate the entire German network with feedback.

We do however, demonstrate the concept using the two-node network governed by the DDE

$$\frac{d^2 \Delta\phi(t)}{dt^2} = 2P_0 - \alpha \frac{d\Delta\phi(t)}{dt} - 2K \sin(\Delta\phi(t)) - \frac{g\alpha}{\tau} (\Delta\phi(t) - \Delta\phi(t - \tau)) u_\tau(t) \quad (52)$$

with $u_\tau(t)$ the Heaviside step function with parameter τ added to avoid any issues with initial conditions. Figure 13 shows a two-node system initialized outside the stability basin of the uncontrolled system ($g = 0$). Without any gain, the system converges to a limit cycle. As gain is increased, it seems that the amplitude of the limit cycle frequency is reduced and the fluctuation period is increased. As gain is increased further, the system converges to its equilibrium solution.

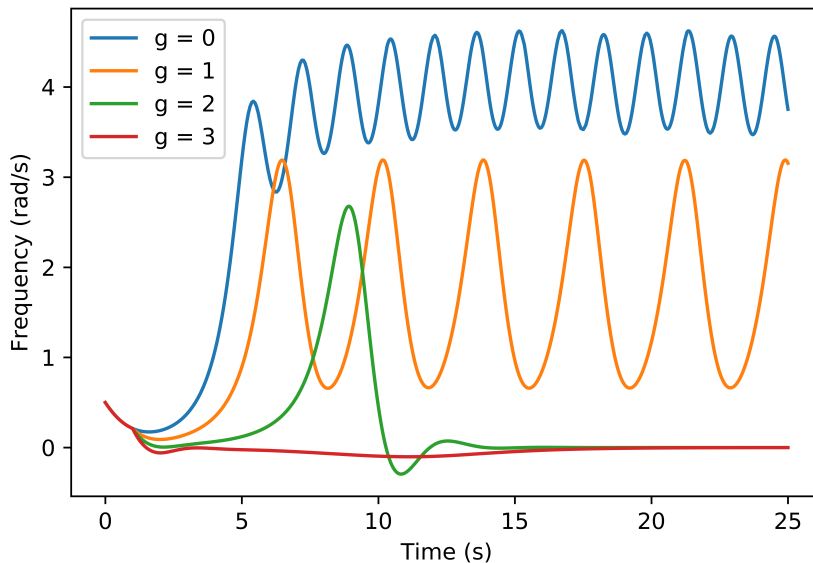


Figure 13: *Frequency plot for various values of g . $P_0 = 1$, $K = 1.1$, $\alpha = 1/2$, $\tau = 1$, $\omega_0 = 0.5$, $\phi_0 = \arcsin(P_0/K) + 0.5$.*

If a system is initialized within the stability basin of the uncontrolled system, it will converge to the stable equilibrium point regardless of the gain. We have shown numerically that for this particular system, the size of the stability basin is indeed increased. In [6] it is shown that the same result holds for the German high power grid, even if feedback is applied to a strict subset of the nodes. We conclude that active feedback systems can indeed help stabilize the grid.

4.2.1 Spectral Analysis

We proceed by analysing the eigenvalues of the linearized version of this two-node system in order to draw conclusions on the existence of stable solutions. This is, however, a bit more involved compared to the two-node system without delay, as it requires solving the transcendental characteristic equation of the form

$$\det(-\lambda I_2 + D_0 + D_\tau e^{-\tau\lambda}) = 0 \quad (53)$$

where D_0 is the Jacobian matrix of the non-delay part of the system of equations and D_τ is the Jacobian matrix of the delayed part. Writing the system as first order equations and considering only the case $t \geq \tau$ we obtain

$$\begin{aligned}\frac{d\omega(t)}{dt} &= 2P_0 - \alpha\omega(t) - 2K \sin \Delta\phi(t) - \frac{g\alpha}{\tau}(\Delta\phi(t) - \Delta\phi(t - \tau)) \\ \frac{d\Delta\phi(t)}{dt} &= \omega(t)\end{aligned}\tag{54}$$

We first consider the equilibrium point $\Delta\phi^* = \arcsin\left(\frac{P_0}{K}\right)$ D_0 has been computed before for the no-gain case, we modify 8 slightly to obtain:

$$D_0 = \begin{bmatrix} -\alpha & -2K\sqrt{1 - \left(\frac{P_0}{K}\right)^2} \\ 1 & 0 \end{bmatrix}\tag{55}$$

And D_τ is easy to compute:

$$D_\tau = \begin{bmatrix} 0 & \frac{g\alpha}{\tau} \\ 0 & 0 \end{bmatrix}\tag{56}$$

Combining equation 53, 55 and 56 gives the characteristic equation:

$$\lambda^2 + \alpha\lambda + \frac{g\alpha}{\tau}(1 - e^{-\tau\lambda}) + 2K\sqrt{1 - \left(\frac{P_0}{K}\right)^2} = 0\tag{57}$$

First order approximation In the small $|\tau\lambda|$ approximation, expanding the exponential to the first order, this simplifies to

$$\lambda^2 + (1 + g)\alpha\lambda + 2K\sqrt{1 - \left(\frac{P_0}{K}\right)^2}\tag{58}$$

which yields

$$\lambda = -\frac{(1 + g)\alpha}{2} \pm \frac{1}{2}\sqrt{((1 + g)\alpha)^2 - 8K\sqrt{1 - \left(\frac{P_0}{K}\right)^2}}\tag{59}$$

and it has previously been shown that in this case $Re\{\lambda\} < 0$. So the solution is indeed stable if τ is small.

Second order approximation Expanding the exponential one step further to the second order, we get

$$\left(1 - \frac{g\alpha\tau}{2}\right)\lambda^2 + (1 + g)\alpha\lambda - 2K\sqrt{1 - \left(\frac{P_0}{K}\right)^2} = 0\tag{60}$$

which we rewrite as

$$\lambda^2 + a\lambda + b = 0\tag{61}$$

with $a = (1 + g)\alpha/(1 - g\alpha\tau/2)$ and $b = 2K\sqrt{1 - \left(\frac{P_0}{K}\right)^2}/(1 - g\alpha\tau/2)$. The resulting eigenvalues are

$$\lambda = -\frac{a}{2} \pm \frac{1}{2}\sqrt{a^2 - 4b}\tag{62}$$

and again, we have a guarantee that $Re\{\lambda\} \leq 0$.

Using similar reasoning, we can conclude that the other equilibrium point $\Delta\phi^* = \pi - \arcsin \frac{P_0}{K}$ is unstable in the first and second order approximation. Note that both approximations are only valid if $\tau\lambda$ is small. This is dependent on all the system parameters and is not a priori known. Thus after computing λ the assumption must be checked.

4.3 Influence of Network Decentralization on the Stability of the Grid

A question of societal interest is how the stability of power grids is influenced by decentralization of the grid. The transition to a sustainable electricity supply includes closing down large coal plants and replacing these by solar parks or wind farms. In the graph model of the power grid this increasing the number of nodes, but keeping the total power generation the same. The question then arises: how does this decentralization influence the stability of the grid?

This question, however, is poorly defined. In previous chapters we have shown that the stability of the grid is dependent on the coupling strength between the nodes, which in turn depends on the power transmission capacity of the cables between the nodes. Thus, in our model of the decentralized network, we need to add an assumption regarding the ratio between the net power production of a node and the coupling strength.

We consider a scenario where one power producing node k with power P_k is replaced by n producers with power P_k/n positioned in a star configuration (from now on: the decentralized network) and then explore the stability of the system by applying normally distributed perturbations to the phases.

4.3.1 Setup

Firstly, it is necessary to set up a decentralized network in a stable equilibrium. Per the results of the chapter on small network analysis, we know the n -producer star network has a stable equilibrium if $\frac{P}{nK} \leq 1$ and in the previous chapter the German high power grid has been shown to have a stable equilibrium point for $K = 1800$ MW. Thus the method used is to initiate both systems in equilibrium and then merge them.

We select the node k from the German high power grid with the highest net power production, subject to the constraint that $P_k \leq \sum_{i=0}^N K_{ik}$. We then set up a n -producer star network, giving the producing nodes power P_{star} such that $nP_{star} = P_k$ and connecting them to a virtual consumer c with power $-P_k$ via cable with capacity K_{star} such that $P_{star}/K_{star} = P_k/\sum_{i=0}^N K_{ik}$. The condition $|P_{star}/K_{star}| < 1$ is satisfied because of the constraint in the node selection.

This process gives two disjoint networks: the German high power grid with $K = 1800$ MW and the n -node star network with n producers connected to a virtual consumer c . In this simulation we take $n = 100$. After setting up both network in stable equilibria, we connect the networks by setting $K_{kc} = K_{ck} = K_{bridge}$, where K_{bridge} is a variable that is slowly increased to a very large value (18000 MW) via an upsweep protocol similar to the one in the previous chapter. If $K_{bridge} \rightarrow \infty$ nodes k and c become fully coupled with $\phi_k = \phi_c$ and total power 0. This means we effectively replace node k by n smaller producers, which is exactly the goal.

4.3.2 Perturbation

We look how the network responds to perturbations by adding a random phase difference to each phase, sampled from a $N(0, \sigma)$ -distribution, simulating for 20 seconds and computing the empirical mean and standard deviation of the frequencies at $t = 20$ s. If the mean and standard deviation are approximately 0, we conclude that the system is again in a stable equilibrium point.

We repeat this procedure 100 times. If the system is less stable, we expect more standard deviations different from 0. The results are for $\sigma = 1$: 6 out of 100 simulations are unstable after 20 seconds with the decentralized network as opposed to 11 out of 100 or the regular German network. While this result seems to indicate that decentralization is beneficial to the stability of the network, the result is statistically insignificant. Fisher's one-sided exact test (computed using python) with $H_0 : p_{decentralized} \leq p_{regular}$,

$H_1 : p_{decentralized} > p_{regular}$ gives a p-value of approximately 0.16, above regularly accepted rejection levels. It is therefore recommendable to repeat this experiment with more repetitions.

5 CONCLUSIONS

In this paper, we used a second order extension of the Kuramoto model to study three power grid stabilizing strategies: increasing the power capacity of the transmission lines between nodes, adding an active feedback system to the nodes and decentralizing. Moreover, we have tested whether examples Braess' paradox, which states that adding an edge in a network can locally improve flow but globally cause congestion, can be found in a small network.

Increasing line capacity We have shown analytically that in a two-node setting increasing the line capacity results in improved stability, in the sense that, assuming a small damping coefficient in the Kuramoto model, there exists a value of the line capacity where the system changes from a state of coexistence between local stability and limit cycles to a state of global stability.

For a more generalized star network consisting of one generator serving equal power to N consumer nodes, we have shown that a stable solution exists provided the transmission line capacity exceeds the transmitted power. So at least increasing the transmission line capacity until that point is sensible.

We have also studied a cyclical network with one generator and N consumers, with all consumers connected to the generator and each consumer connected to its direct neighbor. For the case $N = 3$ we have shown that as the transmission line capacity increases, more equilibrium solutions emerge.

Finally, we considered a model of the real world German power grid and ran simulations using random initial conditions. An important assumption is that all lines have equal capacity. As the line capacity increases, the system becomes stable and all frequencies converge to a very small value. However, between the low capacity regime with existence of limit cycles and the high capacity stable regime there is a medium capacity regime where some nodes have highly fluctuating frequencies. It must be noted, though, that this effect has been observed for just one specific initial state. This is not enough to draw a conclusion about the general size of the stability basin. We have shown that the maximal Lyapunov exponent suddenly goes to zero when the line capacity is increased to a threshold value, indicating indeed that the system becomes stable as the capacity increases.

Active feedback Secondly, we have tested the effect of adding a feedback mechanism to the nodes, where the derivative of the frequency gets an extra counteracting term proportional to the difference between the phase at present time and the phase at some time τ before. This extra term does not give rise to the existence of additional equilibrium solutions, however for the two-node network simulations indicate that the size of the stability basin around stable equilibrium points is increased as one increases the gain factor in the feedback term. We have shown analytically that the (in)stability of the equilibrium solutions is conserved.

Network decentralization Because of the relevance to the development of sustainable grids with solar panels and wind mills, we have simulated the German power grid with one change: the biggest net producing node is replaced by 100 smaller producers with equal power. After bringing the system in an equilibrium state, we have perturbed the initial conditions and ran simulations in order to see if the system would converge to an equilibrium. After 100 simulations on each network, the regular network was unstable 11 times. The decentralized network was only unstable 6 times. While this does hint at a stabilizing effect, the result is statistically insignificant: the p-value is 0.16, above generally accepted rejection criteria. It is therefore recommendable to increase the number of simulations in order to increase the statistical certainty of the result.

Removing a line Braess' paradox predicts that there might exist networks where removing a line from the network has a positive effect on the stability of the grid. Several four-node networks have been investigated, and in all cases the number of equilibrium solutions decreased when a line was removed. Thus we have found no instances of Braess' paradox in the four-node networks. It was unfeasible to compute the size of the stability basins. Therefore, no conclusions can be drawn on the existence of networks where removing a line has a positive effect. Further research could include computing the size of stability basins in order to draw conclusions about the effect of line removal.

LIST OF REFERENCES

References

- [1] J. Deign, “Germany’s maxed-out grid is causing trouble across europe,” Mar 2020.
- [2] E. Bellini, “Netherlands grid constraints becoming serious threat to solar,” Nov 2019.
- [3] K. Appunn, “Energiewende hinges on unblocking the power grid,” Apr 2018.
- [4] P. Capros *et al.*, *EU Reference Scenario 2016*. Publications office of the European Union, 2016.
- [5] D. Manik, D. Witthaut, B. Schäfer, M. Matthiae, A. Sorge, M. Rohden, E. Katifori, and M. Timme, “Supply networks: Instabilities without overload,” *The European Physical Journal Special Topics*, vol. 223, no. 12, p. 2527–2547, 2014.
- [6] H. Taher, S. Olmi, and E. Schöll, “Enhancing power grid synchronization and stability through time-delayed feedback control,” *Physical Review E*, vol. 100, Aug 2019.
- [7] M. Rohden, A. Sorge, M. Timme, and D. Witthaut, “Self-organized synchronization in decentralized power grids,” *Physical Review Letters*, vol. 109, Aug 2012.
- [8] S. Sastry, *Nonlinear systems: analysis, stability, and control*. Springer, 1999.
- [9] E. I. Pas and S. L. Principio, “Braess’ paradox: Some new insights,” *Transportation Research Part B: Methodological*, vol. 31, no. 3, p. 265–276, 1997.
- [10] J. Ergerer, *Open Source Electricity Model for Germany (ELMOD-DE)*. Deutsches Institut für Wirtschaftsforschung, 2016.
- [11] M. Cencini, F. Cecconi, and A. Vulpiani, *Chaos: from simple models to complex systems*. World Scientific, 2010.